Aerosol retrievals and measurements from space

Jun Wang

ARROMA group

Aerosol, Radiation, Remote-sensing, & Observation-based Modeling of Atmosphere

Univ. of Nebraska

Univ. of Iowa, starting Aug 2016

NCAR ASP Summer Colloquium
Advances in Air Quality Analysis and Prediction
The Interaction of Science & Policy
July 25 - August 5, 2016

Outline

- Introduction to aerosol properties
- Aerosol retrieval with one channel (wavelength)
- Aerosol retrieval with two channels (wavelengths)
- Aerosol retrieval with multiple channels
- Aerosol retrieval with polarization
- Application of satellite-based aerosol data for surface PM2.5
- Future directions

Origin of aerosols

Primary sources:
directly from surface

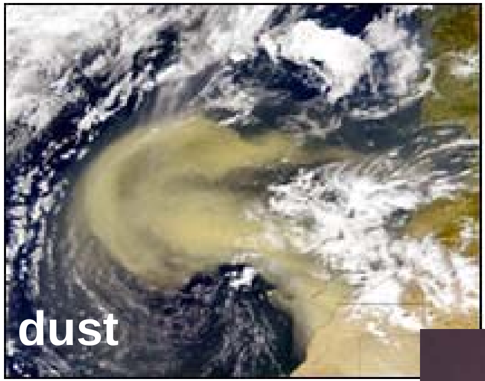

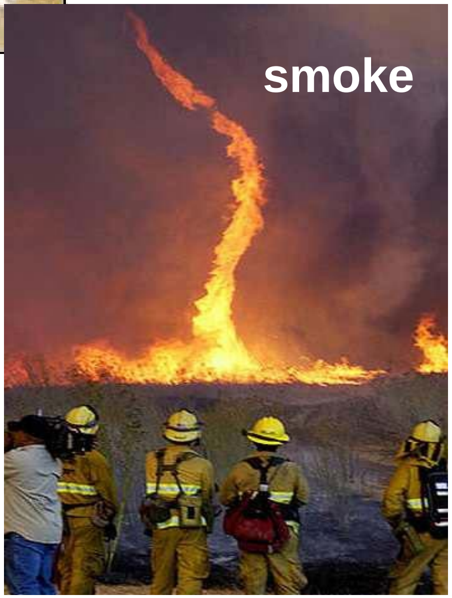

Secondary sources:
Atmospheric chemistry

Aerosols have large spatiotemporal variations (minutes-hours, meters to kilometers).

Life cycle and importance of tropospheric aerosols

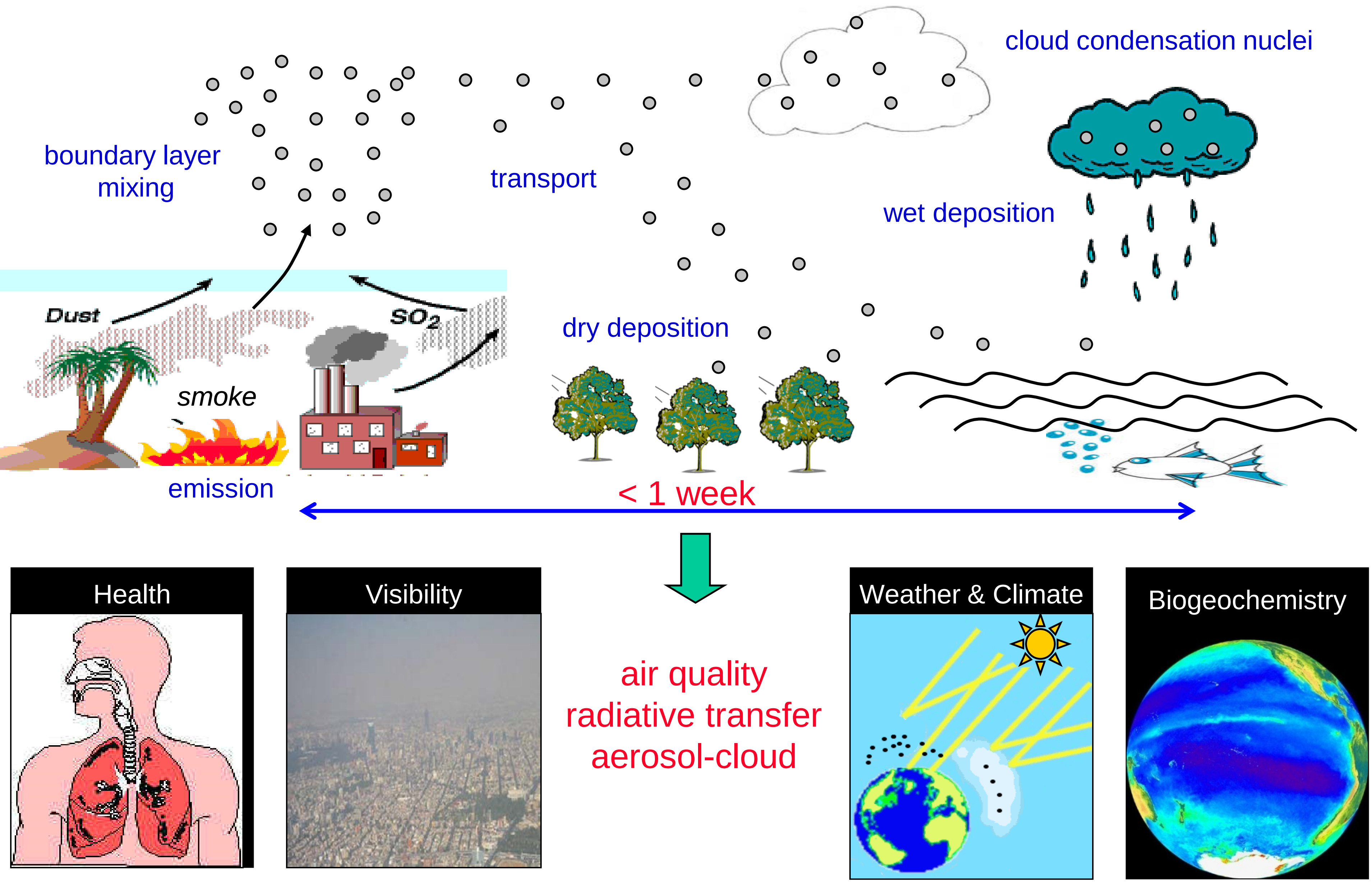

MODIS global true color image
25 July 2016

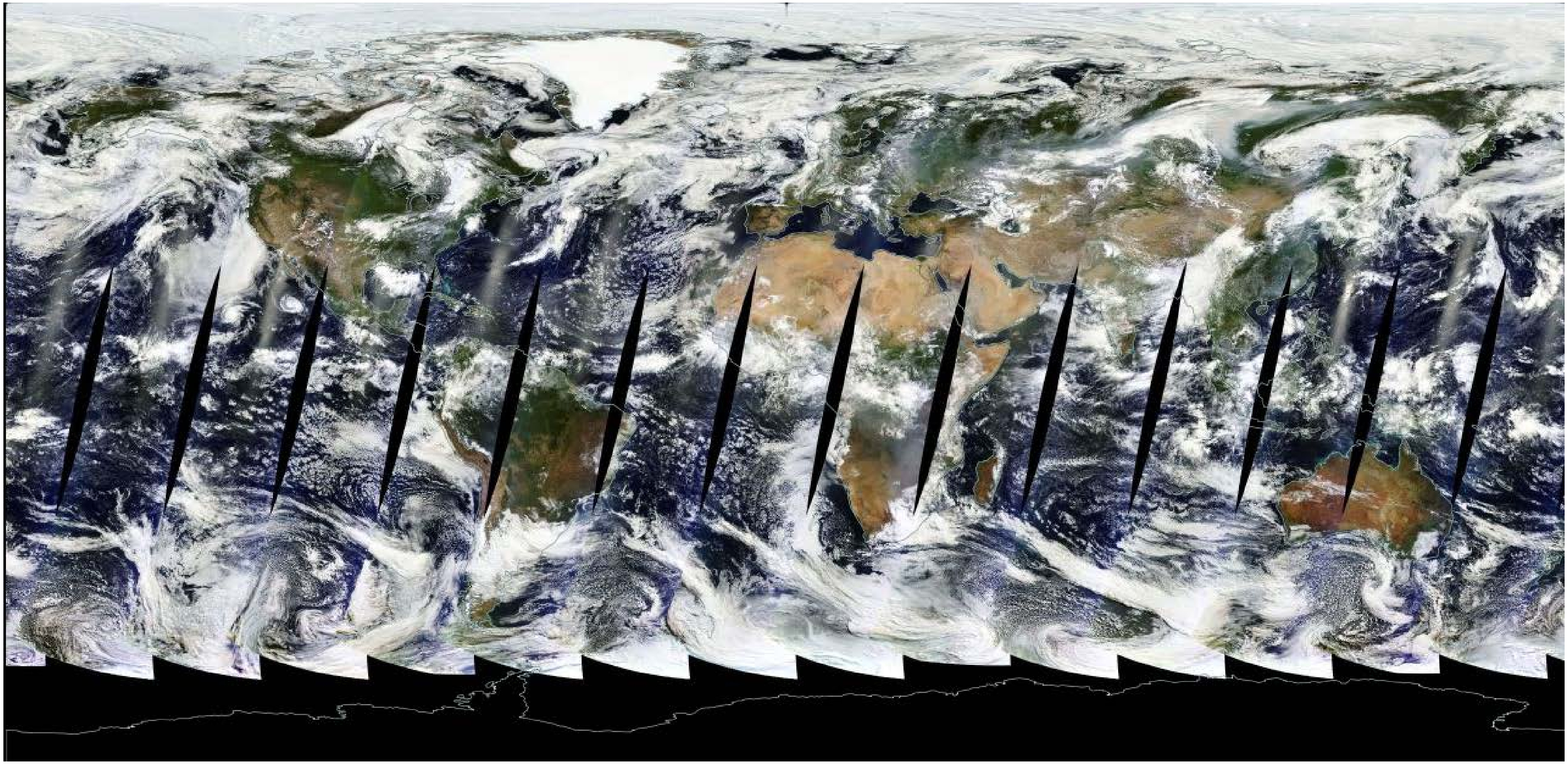

Clouds: White ; Bare soil: Yellowish; Canopy: Green; Ocean: dark

What is the color of an aerosol layer?

https://worldview.earthdata.nasa.gov/

Aerosol observation from space by solar backscatter

Dust

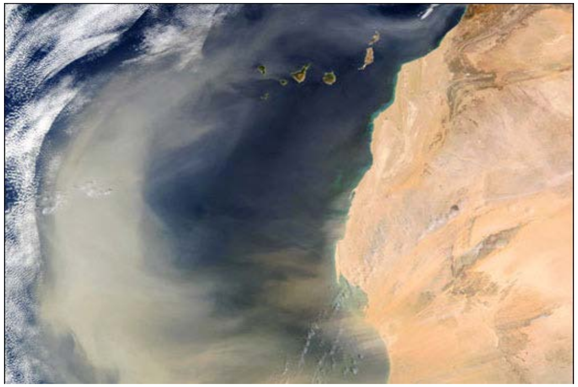

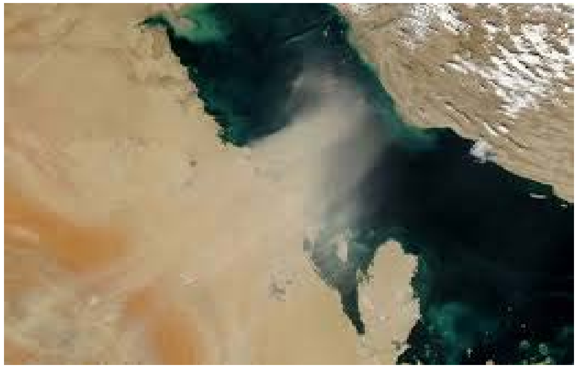

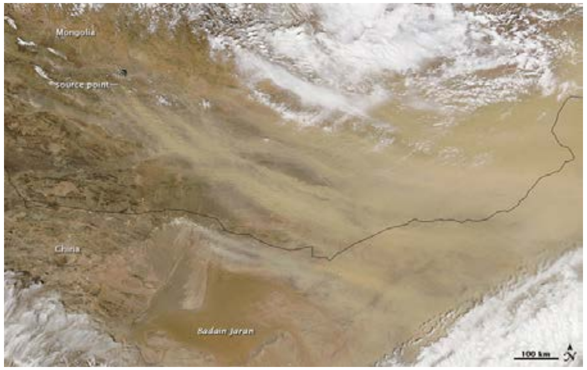

Smoke

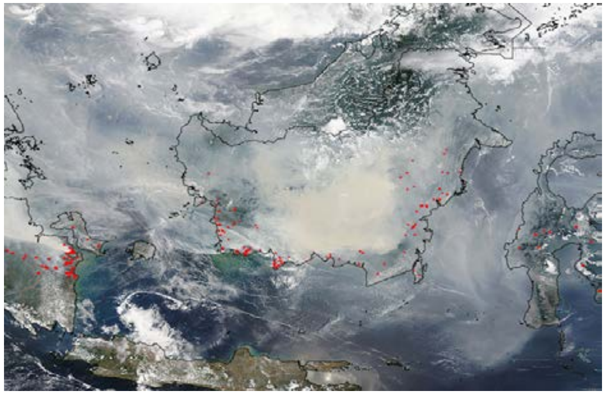

Haze

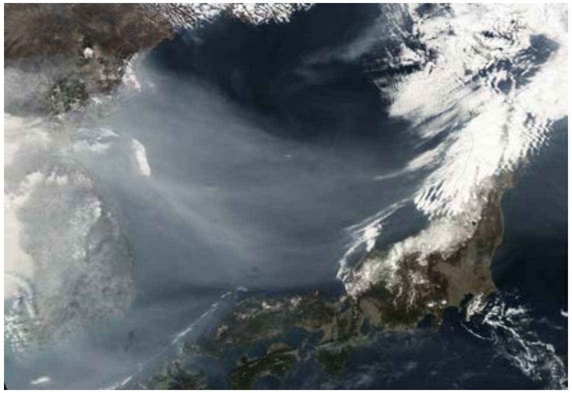

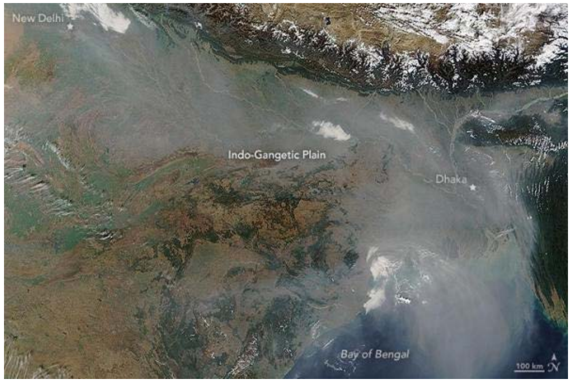

Scattering regimes

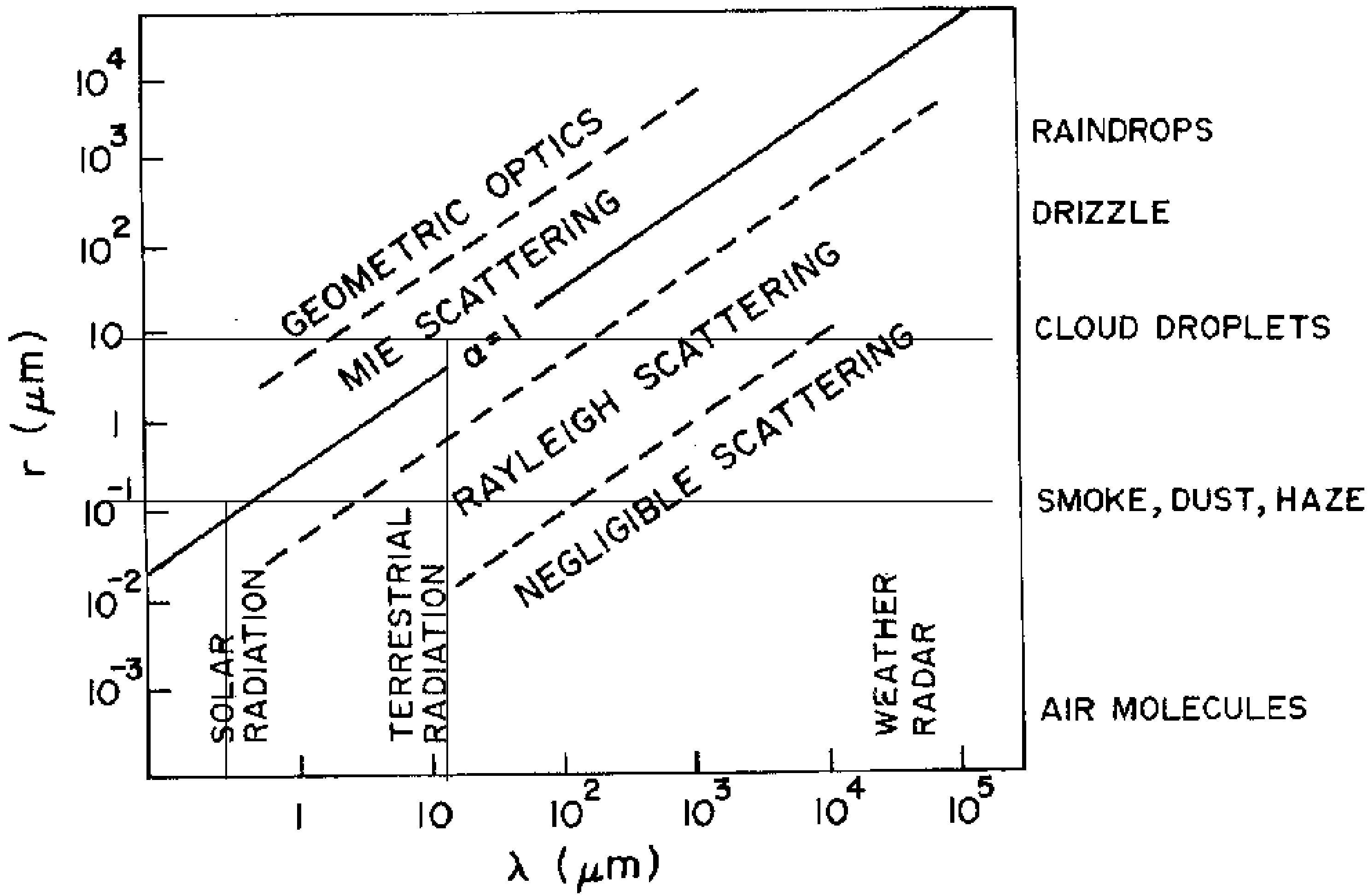

The scattering of solar and terrestrial radiation by atmospheric aerosols and clouds is mostly in the Mie scattering regime.

Aerosol scattering of solar radiation depends on

Radiative/Optical properties

Physical Properties

***1st order* relationship**

- **Aerosol Optical Depth** τ ← **Atmospheric loading of aerosol mass**
- **Single Scattering albedo** ω ← **Refractive index of aerosol particles**
- **Phase Function** $P(\Theta)$ ← **Size distribution of aerosol particles**; **Shape/morphology of aerosol particles**

The chemical composition of aerosols highly vary in space & time;
So do aerosol optical properties.

We can not obtain all aerosol properties from space.

The parameter commonly retrieved with good accuracy:

Aerosol Optical Depth (AOD) or Aerosol Optical Thickness (AOT) or τ

$$I = I_0 \, e^{-\tau/\cos(\theta)}$$

Beer's law:

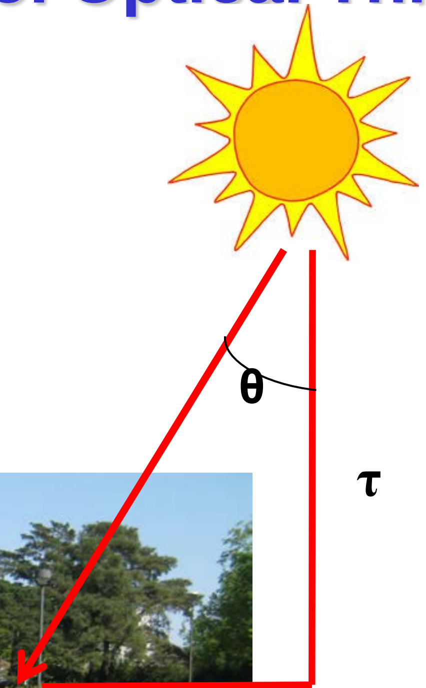

Phy. Met. class

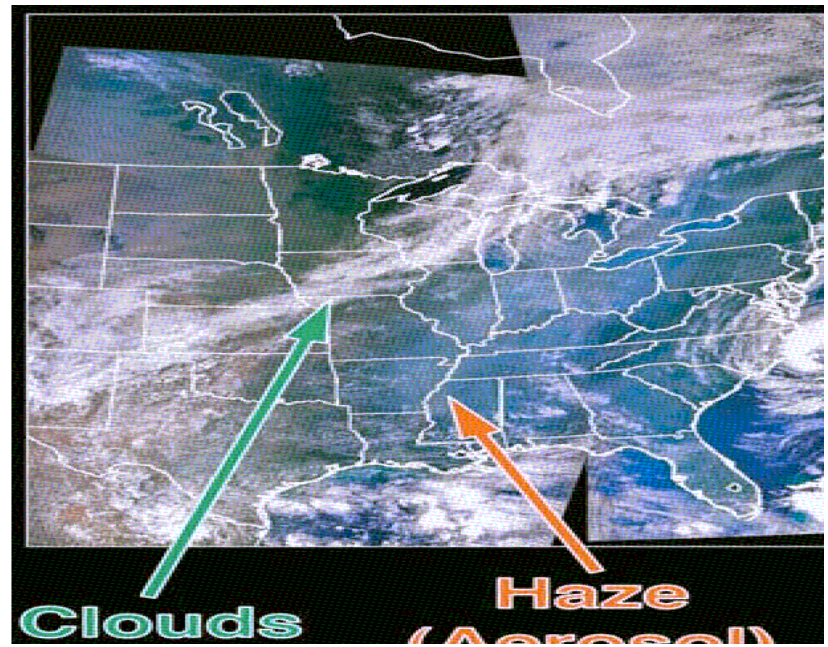

τ is generally retrieved from satellite visible channels over clear sky conditions (Wang et al., 2003).

Retrieval of AOD from one channel

single scattering, low R_{sfc} (<0.1)

Key factors : ω, P(θ), and R_{sfc}

Refractive index, Size, Shape, etc

$$R_{sat} = R_{sfc} + \frac{\omega \tau P(\theta)}{4 \mu \mu_0}$$

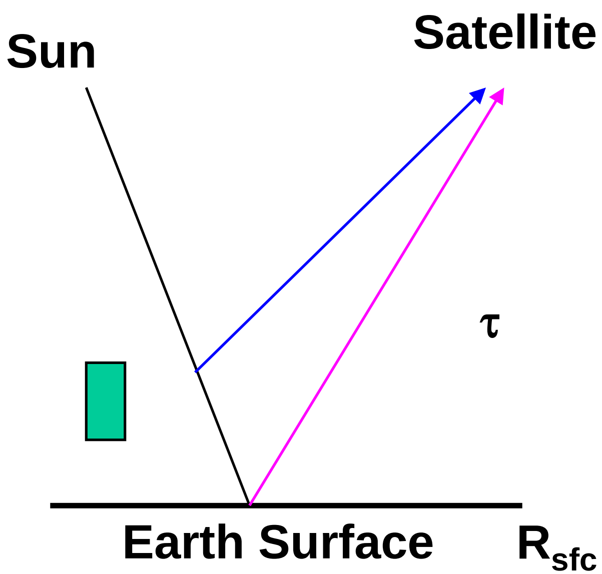

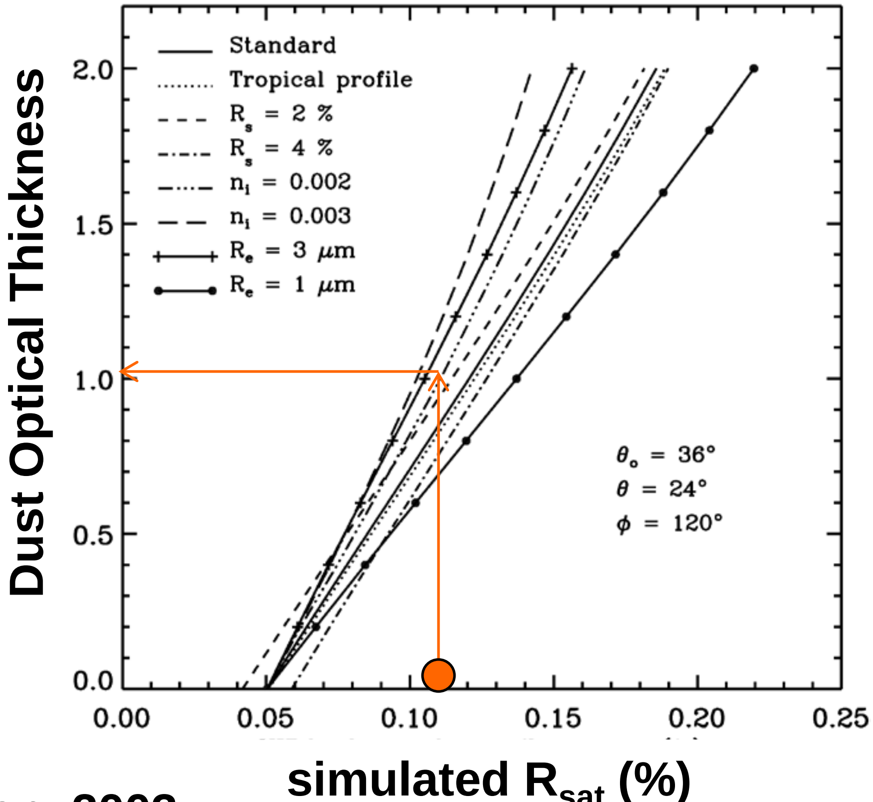

Liu, Wang & Christopher, Int. J. Rem. Sen.,2003

AOD from AVHRR

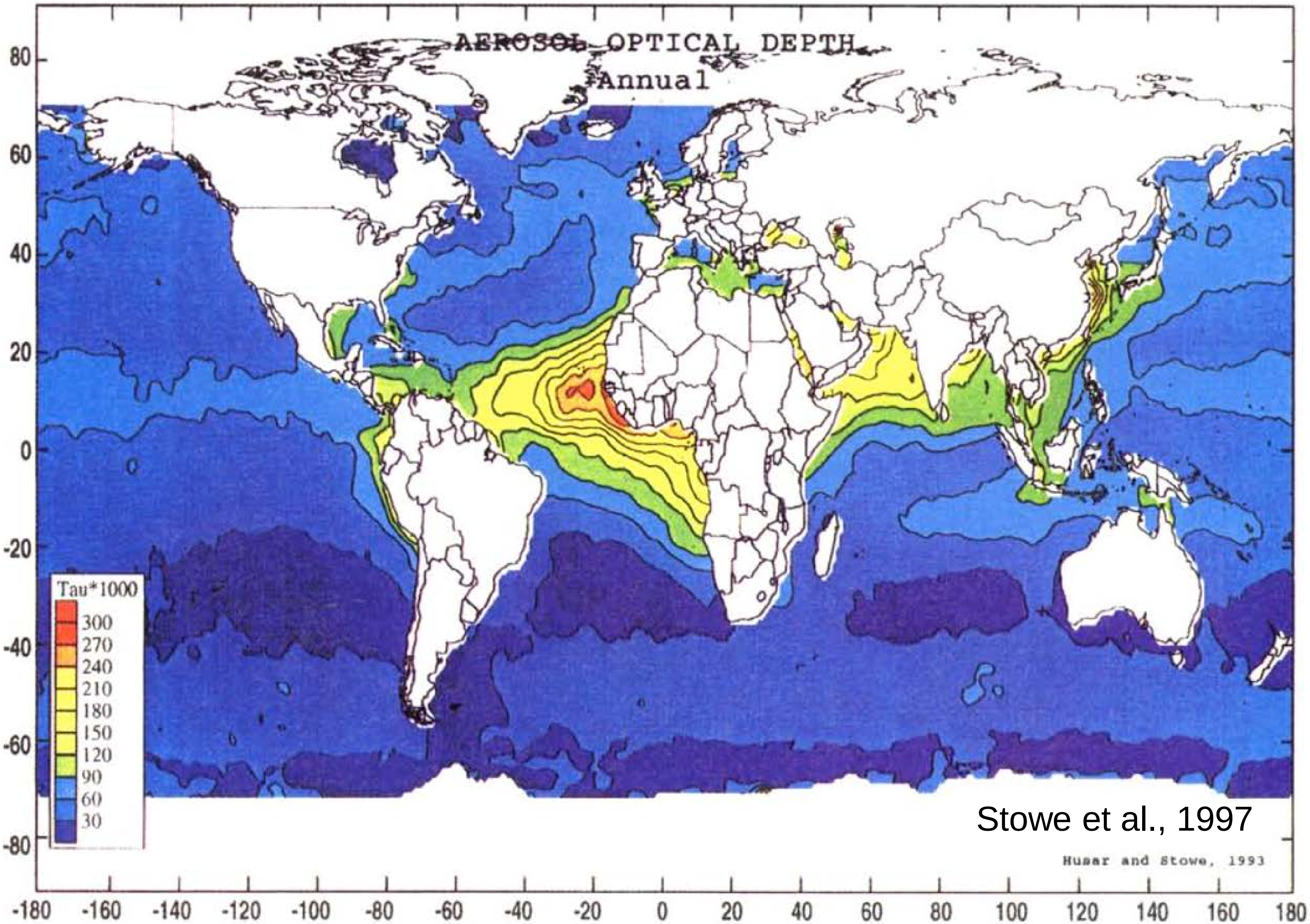

Plate 2. Mean distribution of τ^{A}_{SAT1} at 0.5 μm for 2 years prior to the eruption of Mount Pinatubo.

The retrieval has very large uncertainties

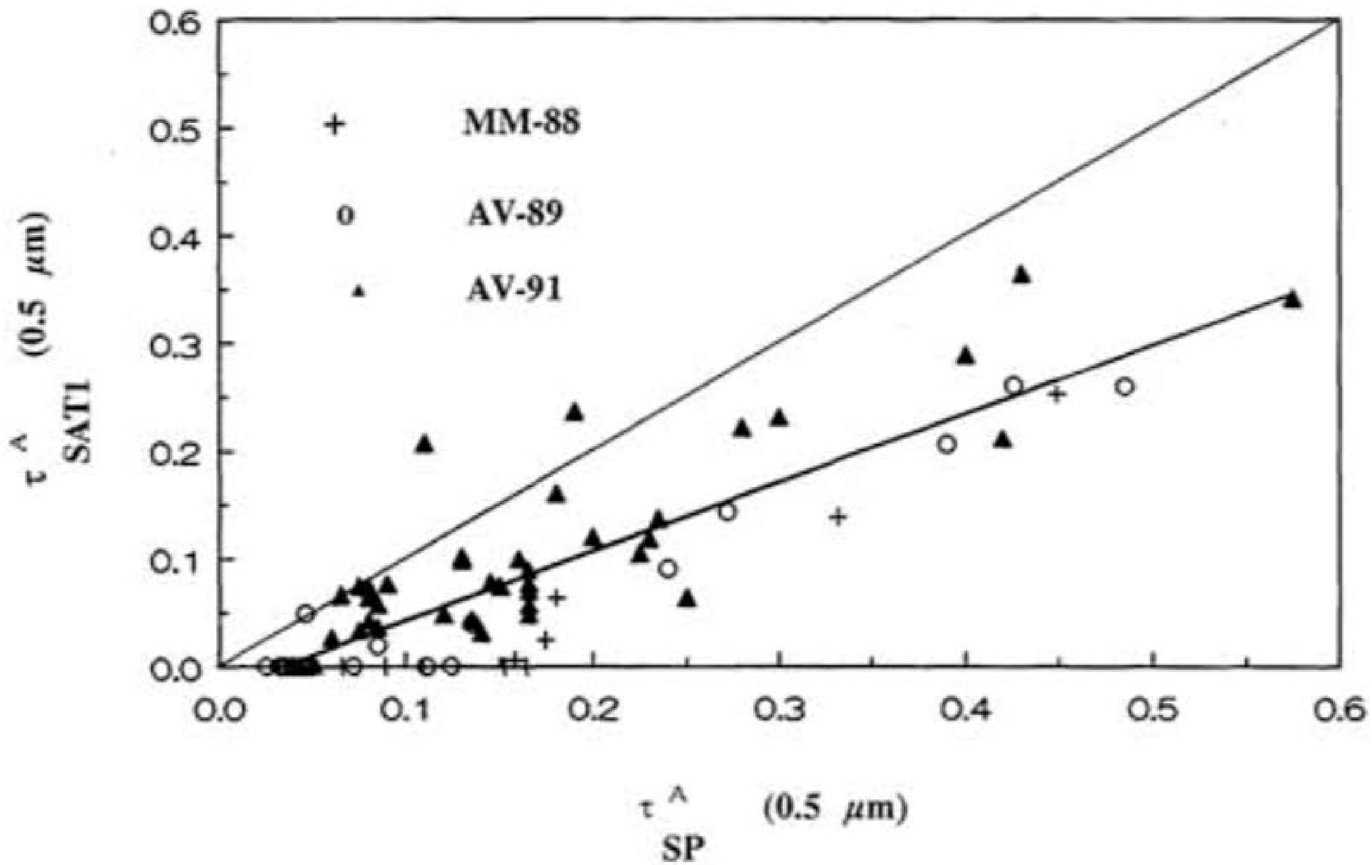

Figure 2. Regression of τ^{A}_{SAT1} against Sun-photometer aerosol optical thickness at 0.5-μm wavelength.

Two – channel retrieval algorithm

Wavelength dependence can be used as an indicator to the aerosol size

Angstrom's [1929] empirical expression is given

$$\tau_a = \beta\lambda^{-\alpha} \qquad (1)$$

Eck et al., JGR, 1999

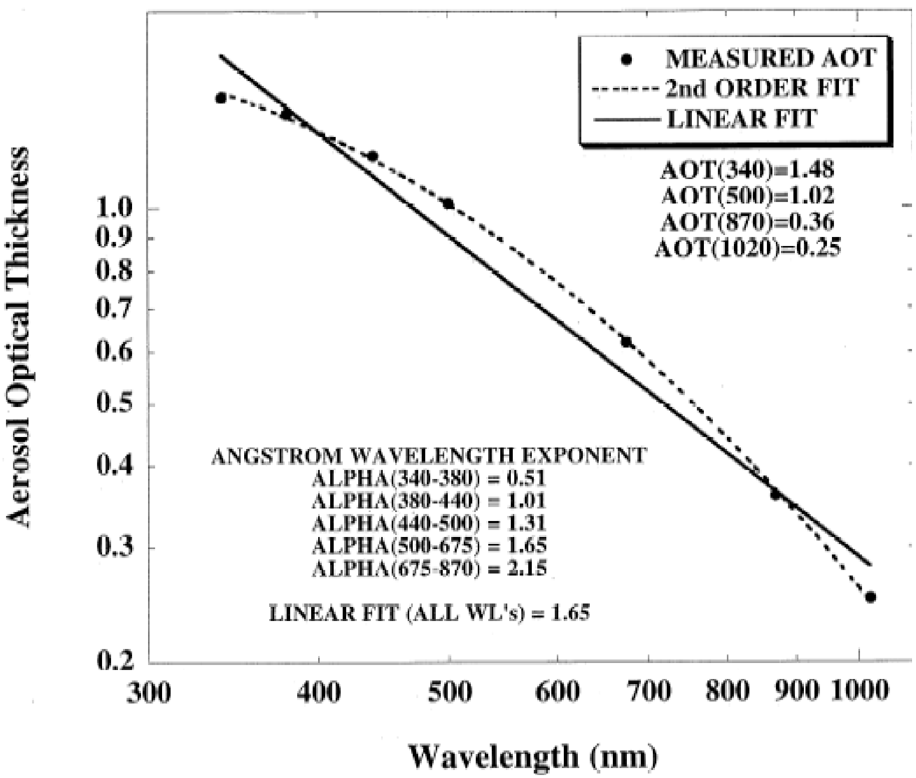

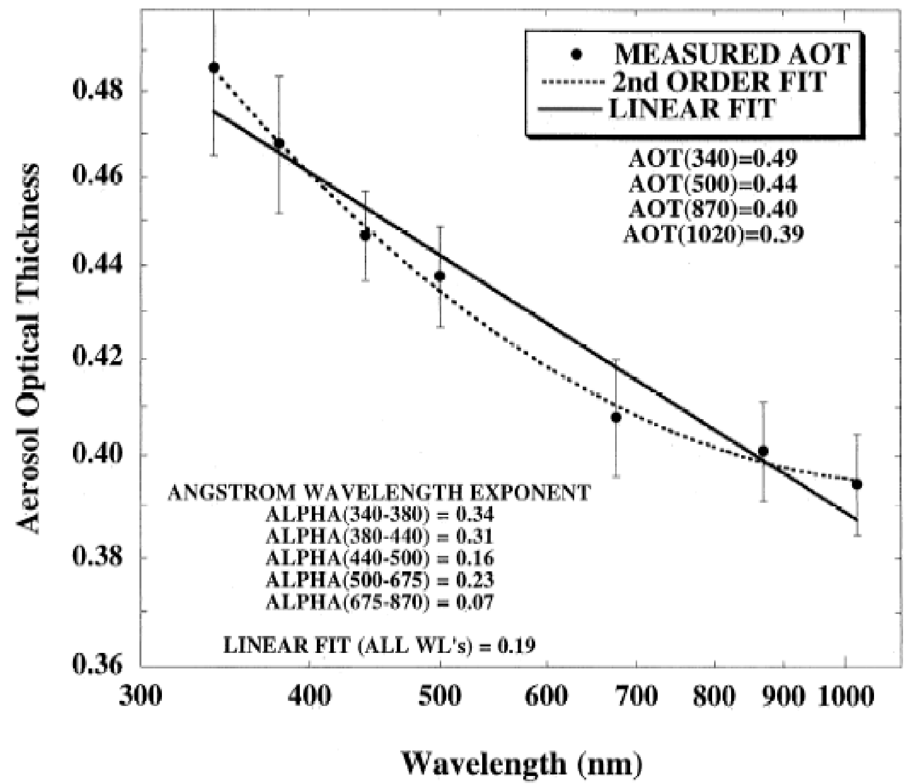

Urban aerosols in Washing DC

Dust aerosols in Mongolia

AOD retrieval from AVHRR two channels

Anthropogenic particle, smaller size

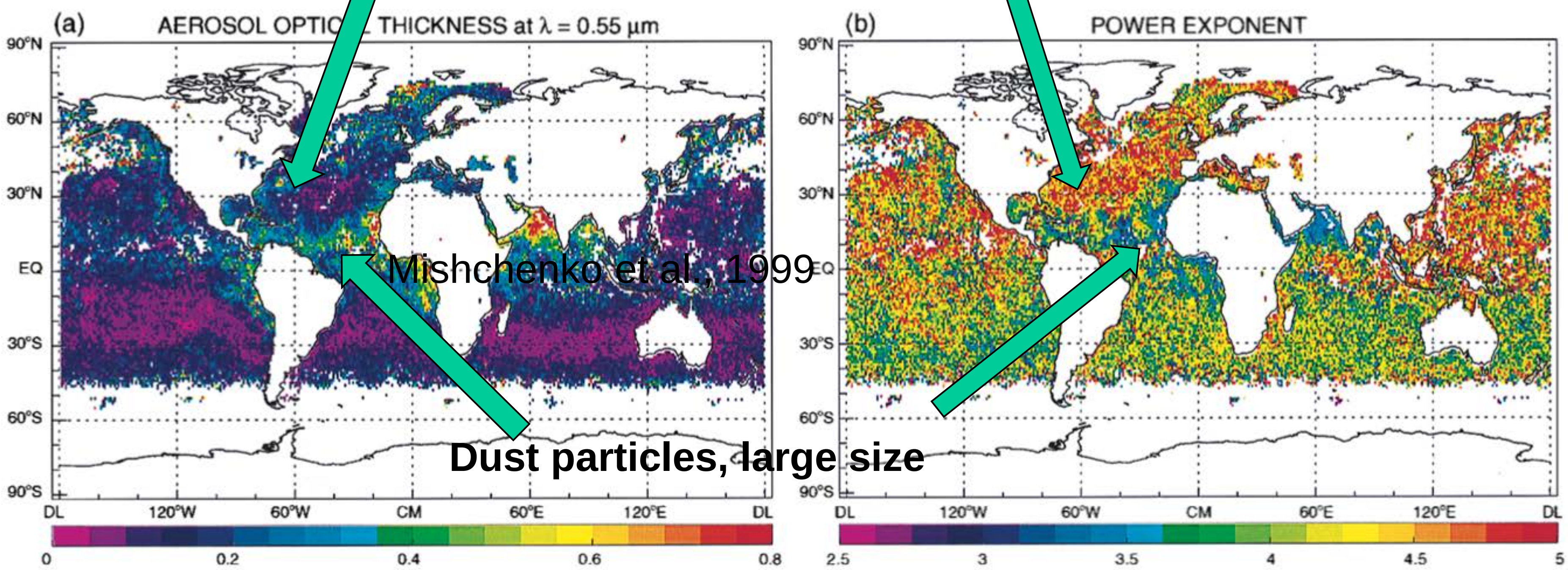

Dust particles, large size

Mishchenko et al., 1999
Ignatov et al., 1998.

The larger the wavelength dependence of AOD, the smaller the particle size

Challenges: land surface reflectance

$$R_{sat} = R_{sfc} + \frac{\omega\tau P(\theta)}{4\mu\mu_0}$$

Only valid when Rsfc is small.

Kaufman and Fraser, 1985

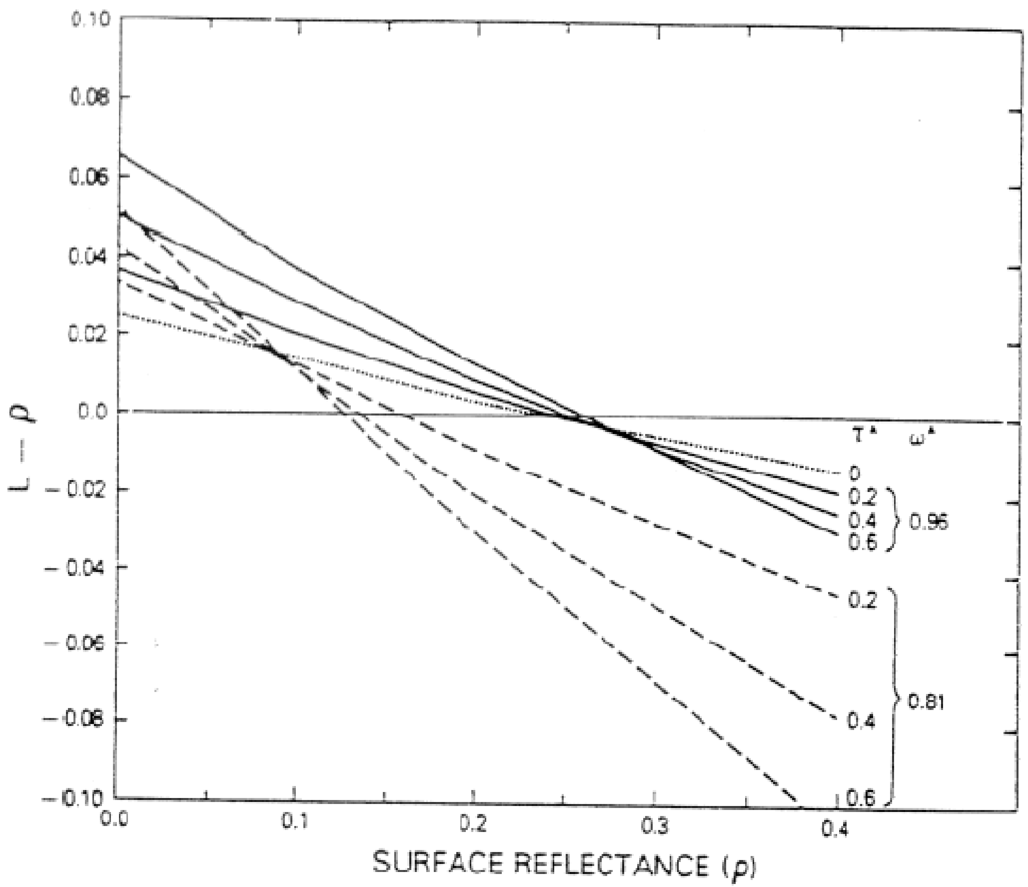

Reflectance over ocean is low and relatively homogenous.

When surface gets brighter, aerosol absorbs more light reflected by the surfaces, thereby reducing the surface vs. top-of-atmosphere contrast; not favorable for retrieval.

Aerosol Effects on Reflected Solar Radiation over Land

Biomass burning
Cuiabá, Brazil (August 25, 1995)

R = 0.66 µm
G = 0.55 µm
B = 0.47 µm

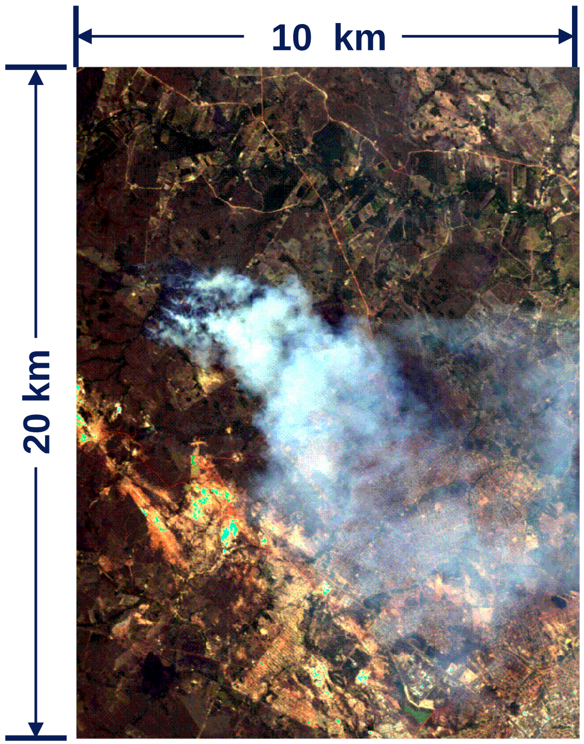

θ_0 = 36°

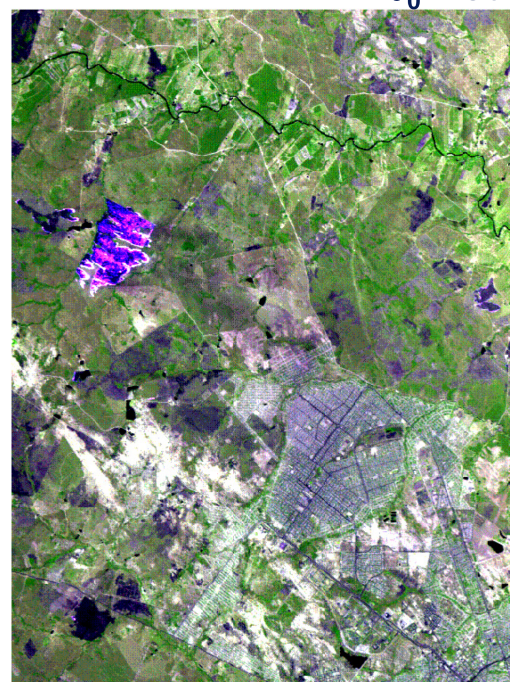

R = 1.65 µm
G = 1.2 µm
B = 2.1 µm

Smoke signal is weaker in NIR

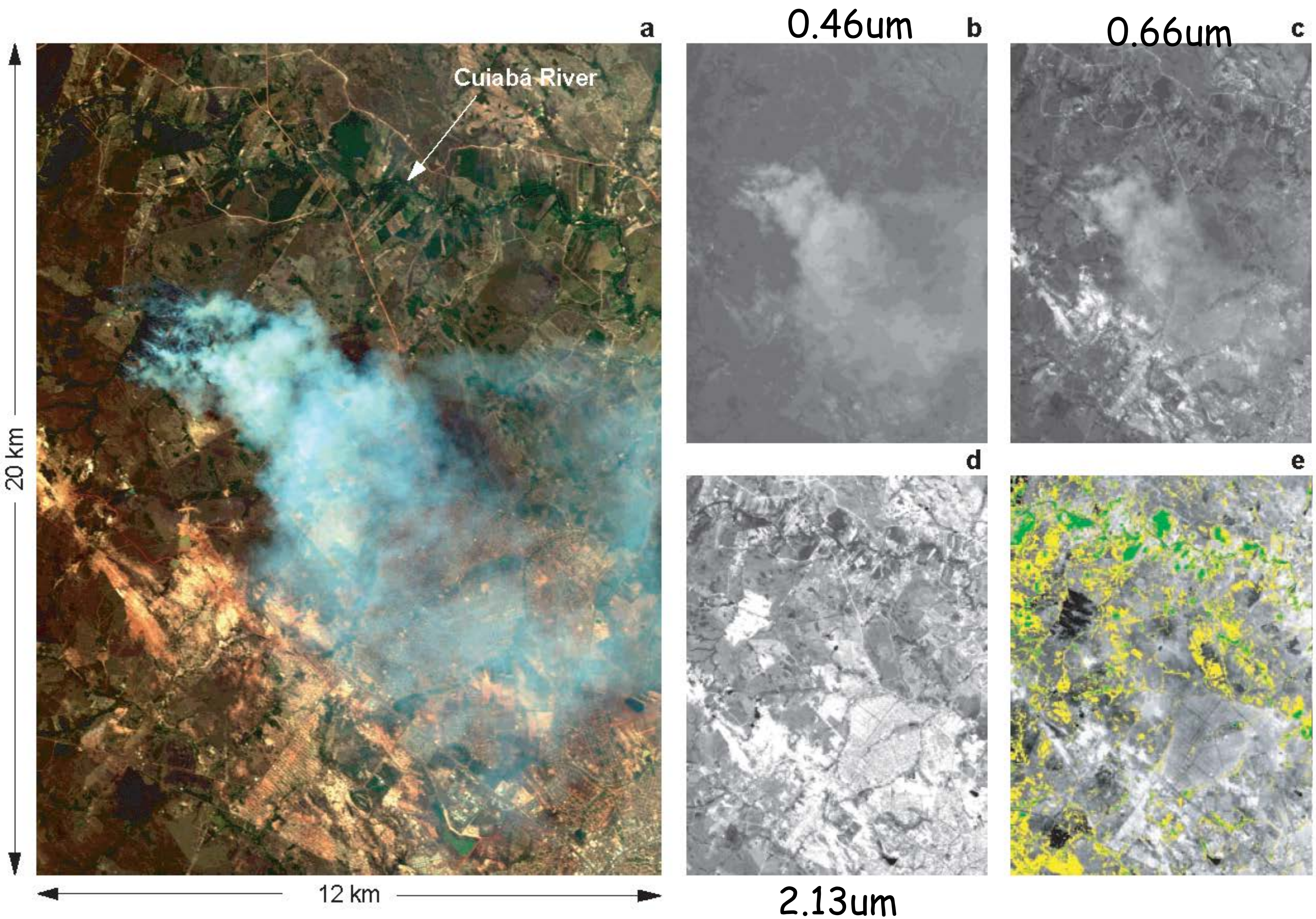

King et al., BAMS, 1999

Using NIR reflectance to derive VIS

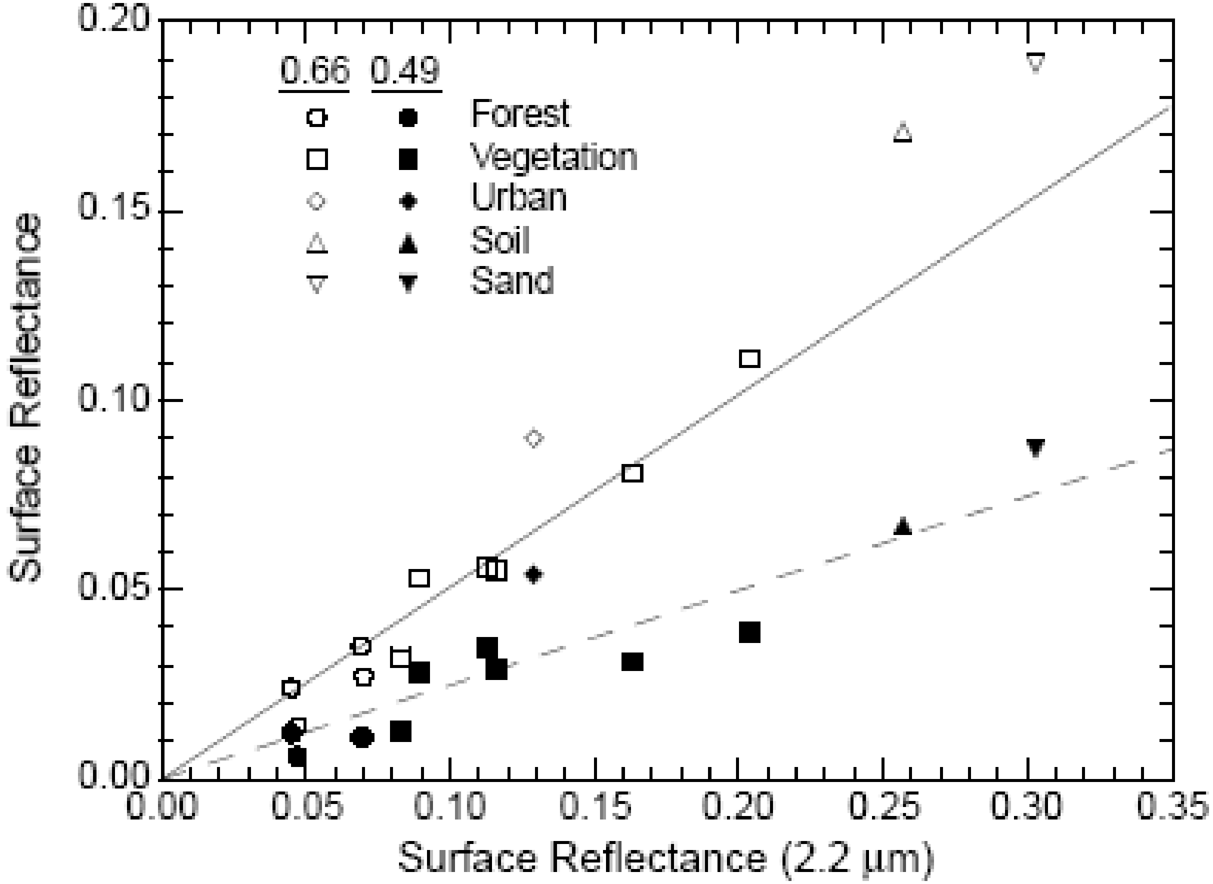

$A_g(0.47\ \mu m) = 0.5\ A_g(0.66\ \mu m)$

$= 0.25 A_g(2.1\ \mu m)$

How aerosol optical properties are calculated?

Remer et al., 2005

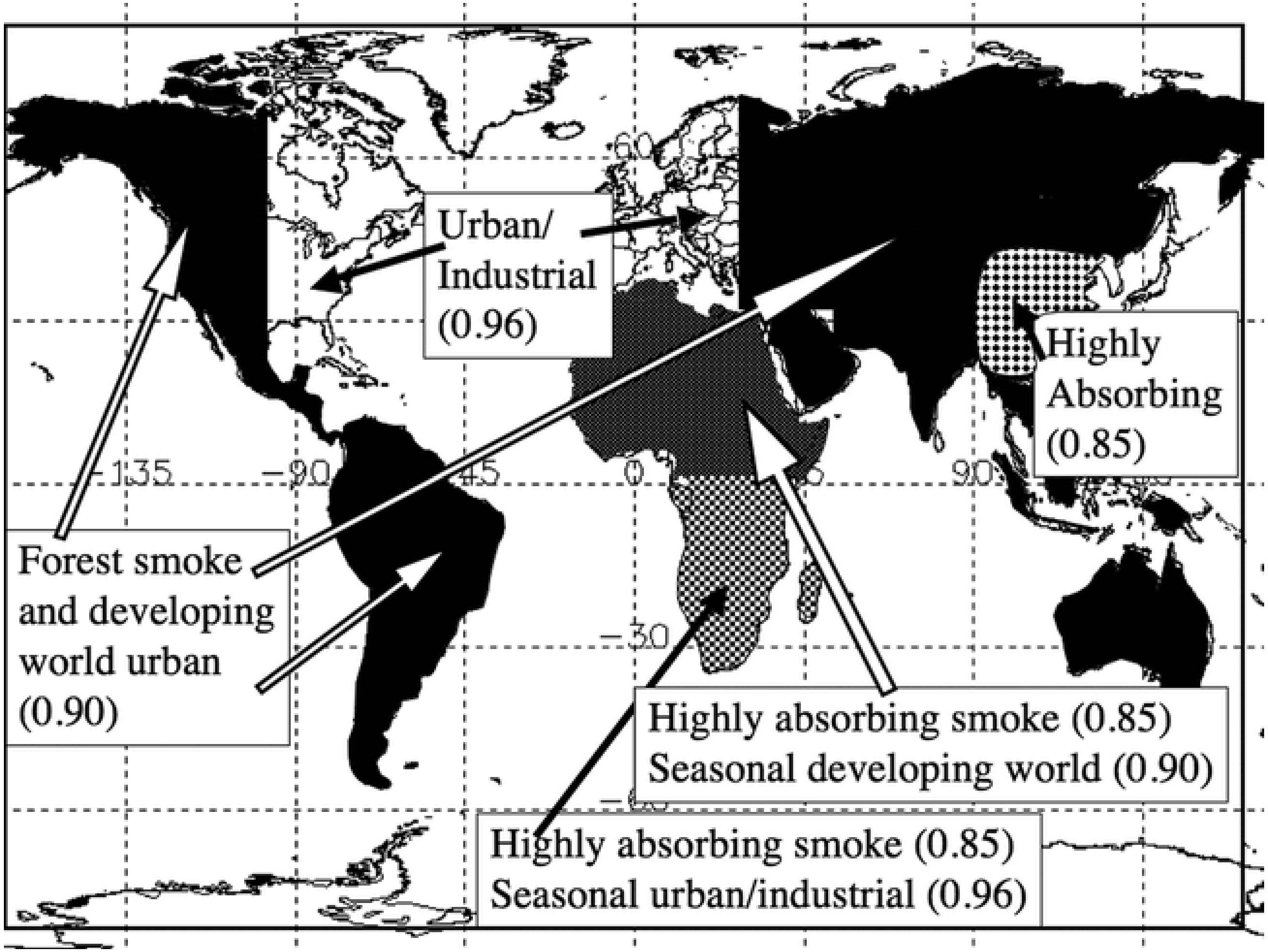

The selection of aerosol optical model primarily is primarily based on geographical locations.

Lastest version of aerosol climatology in MODIS retrieval (Levy et al., 2013)

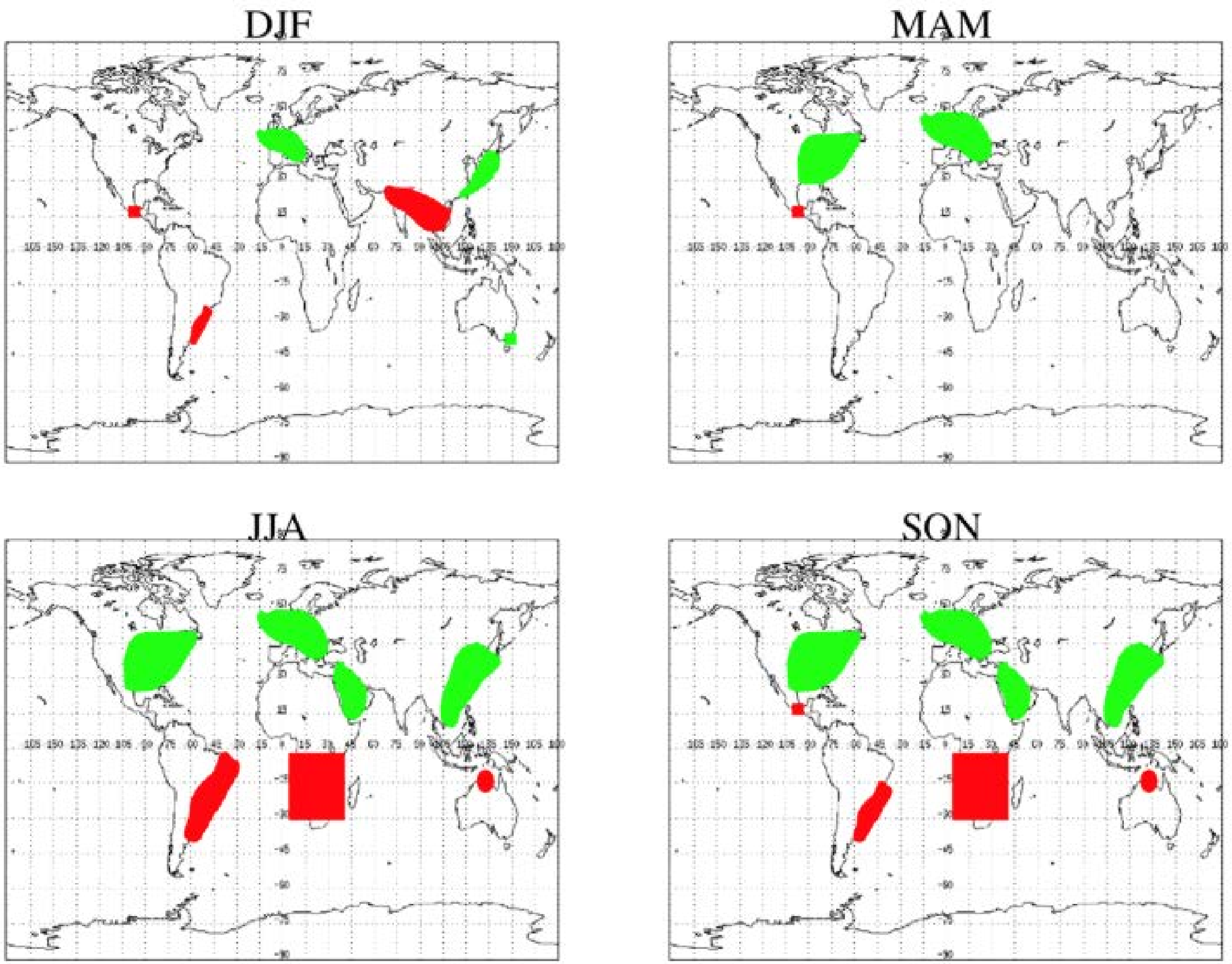

Red and green: absorbing (SSA ~0.85) or nonabsorbing (SSA~ 0.95). Moderately absorbing (SSA~ 0.90) is assumed everywhere else.

MODIS AOD

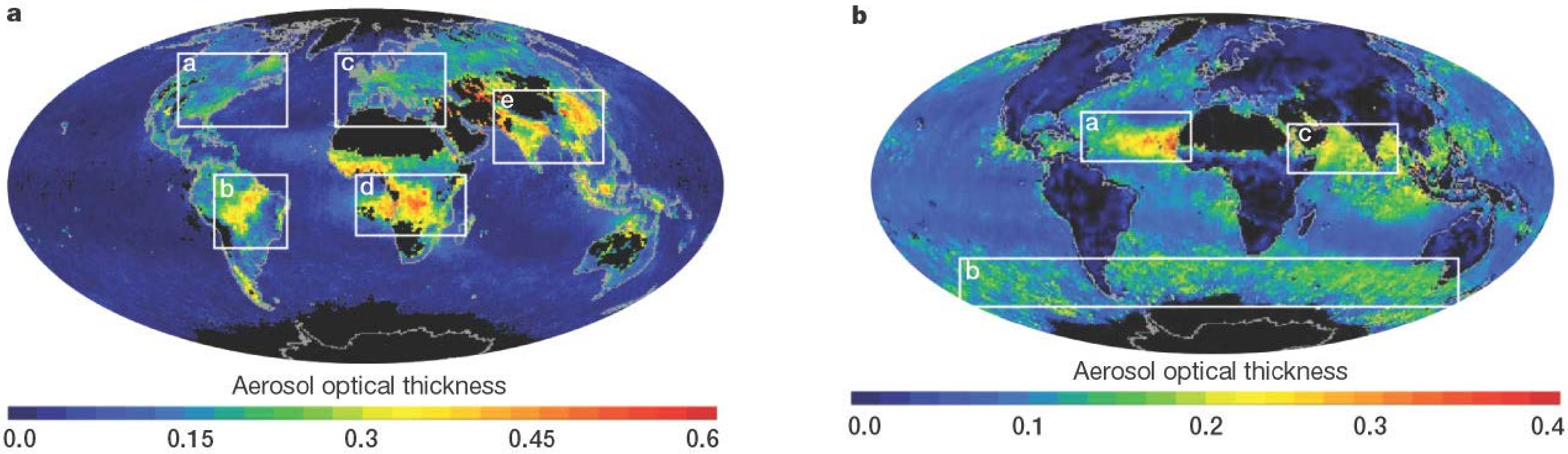

MODIS AOD. (a) fine mode AOD ; (b) coarse mode AOD, September 2000

Validation of AOD

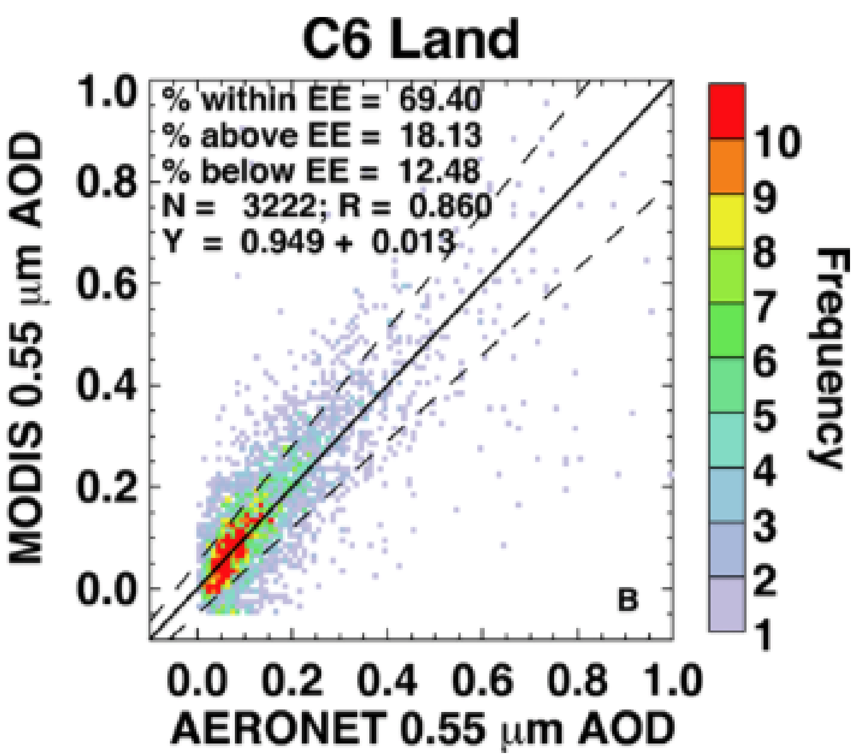

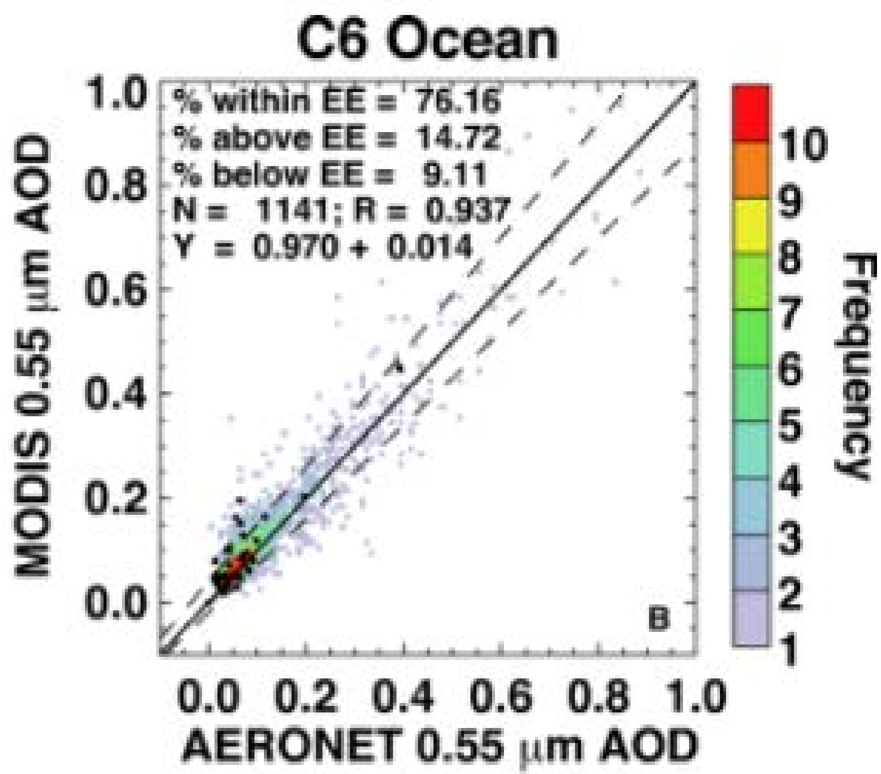

Validation of Angstrom exponent over ocean only; overland is not recommended to use

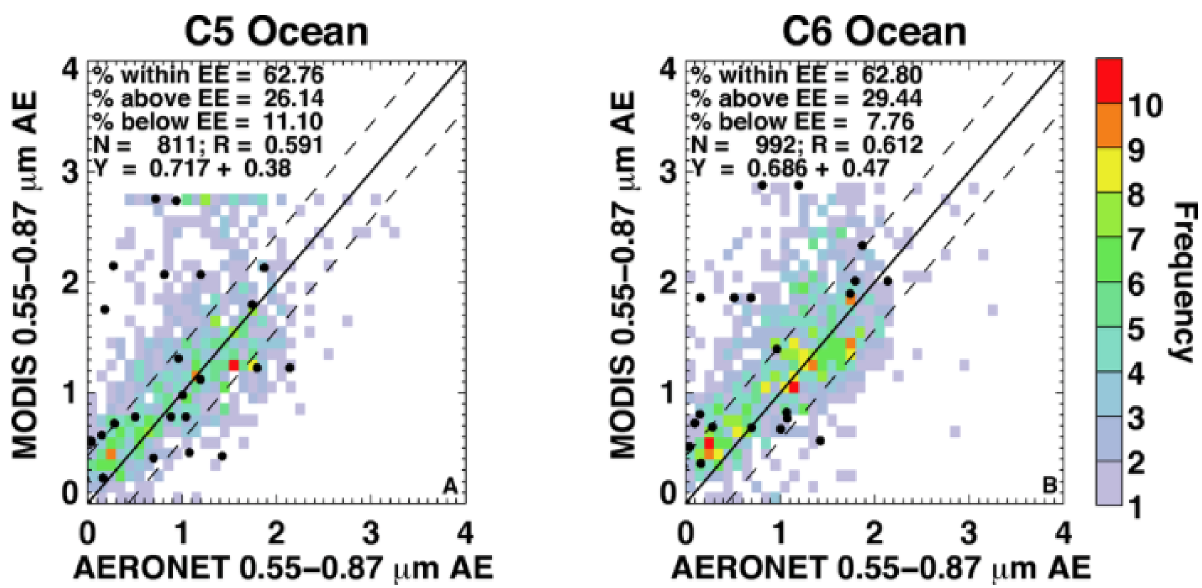

Fig. 17. Frequency scatter plots for AE at 0.55/0.86 μm over DT-ocean compared to AERONET (gray and color dots) and MAN (black dots), plotted from 6 months of Aqua (January and July; 2003, 2008 and 2010), computed with C5 algorithm **(a)** and C6 algorithm **(b)**. One-one lines and EE envelopes (±0.45) are plotted as solid and dashed lines. Collocation statistics are presented in each panel.

Global map of AOD

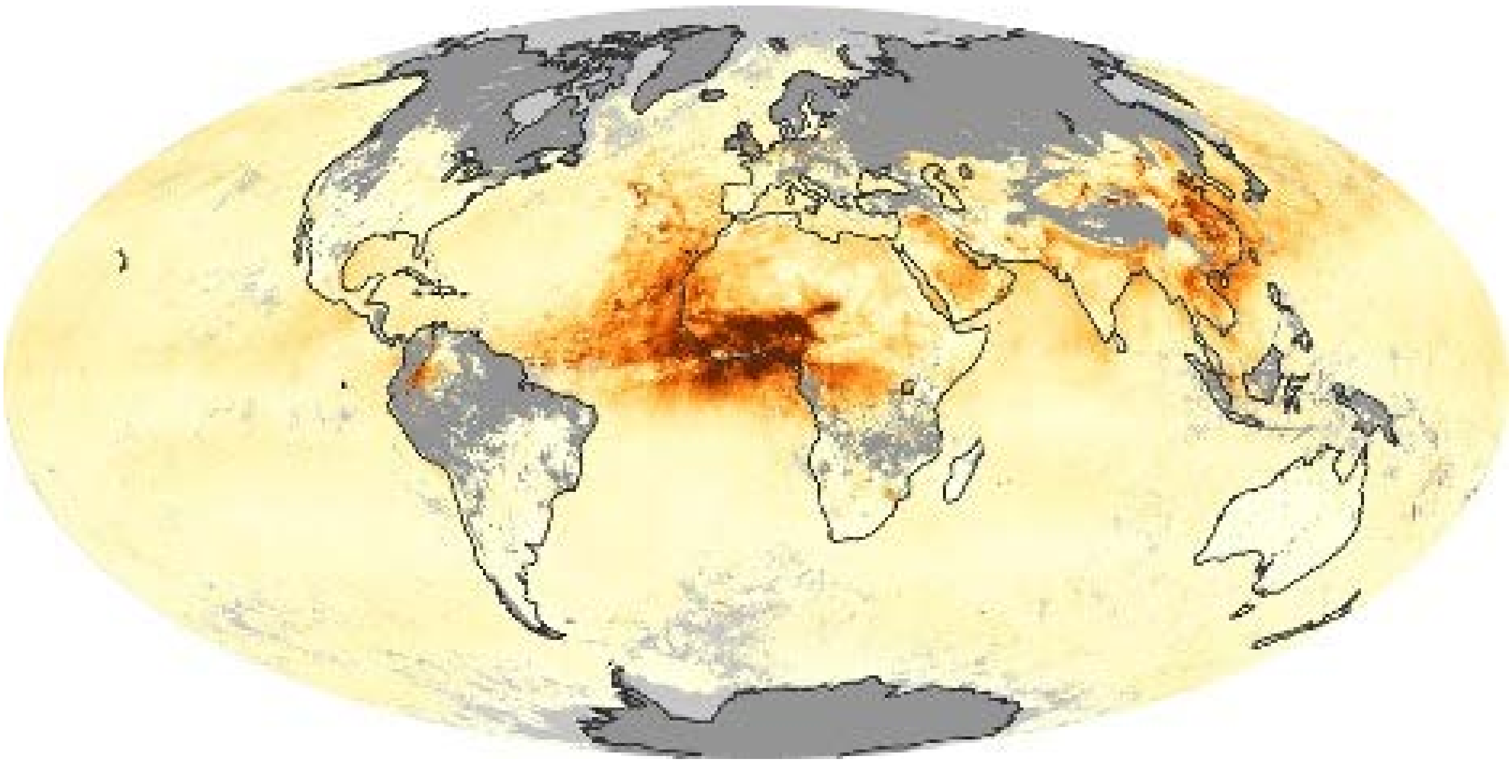

Deep-blue algorithm (Hsu et al., 2013) and Dark-target algorithm (Levy et al., 2016)

MISR Imaging SpectroRadiometer   MISR

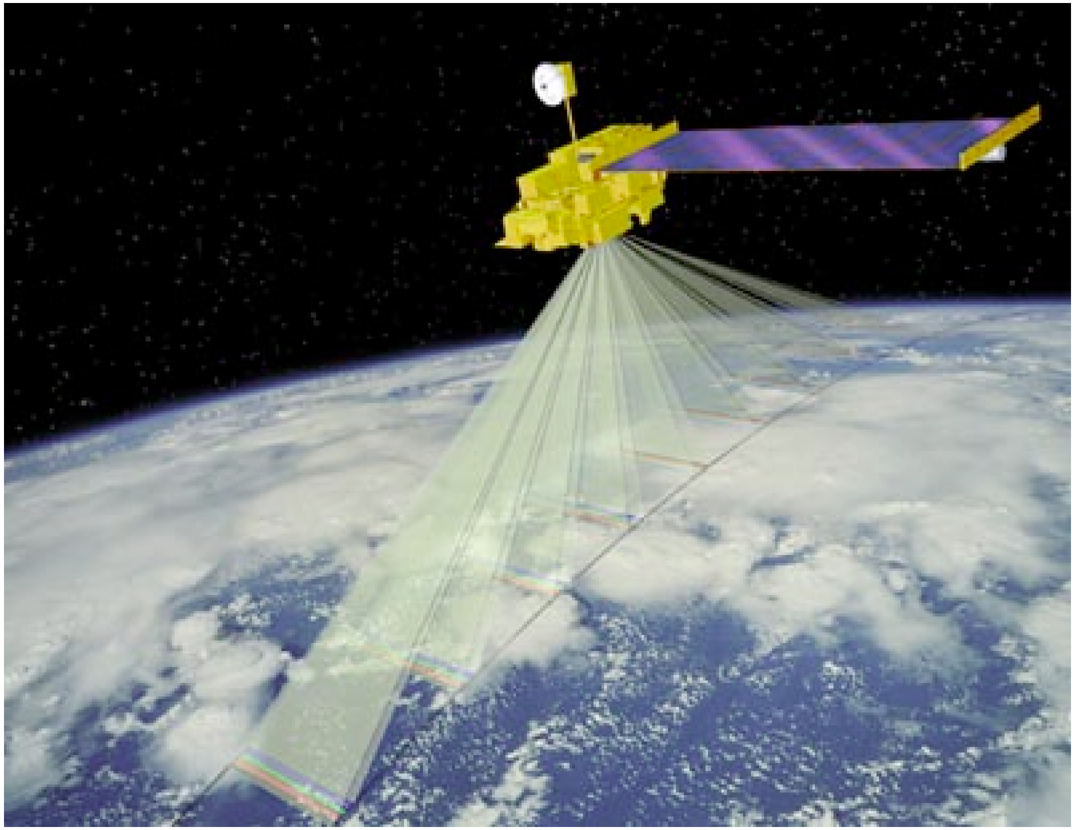

Enhancing sensitivity to thin aerosols

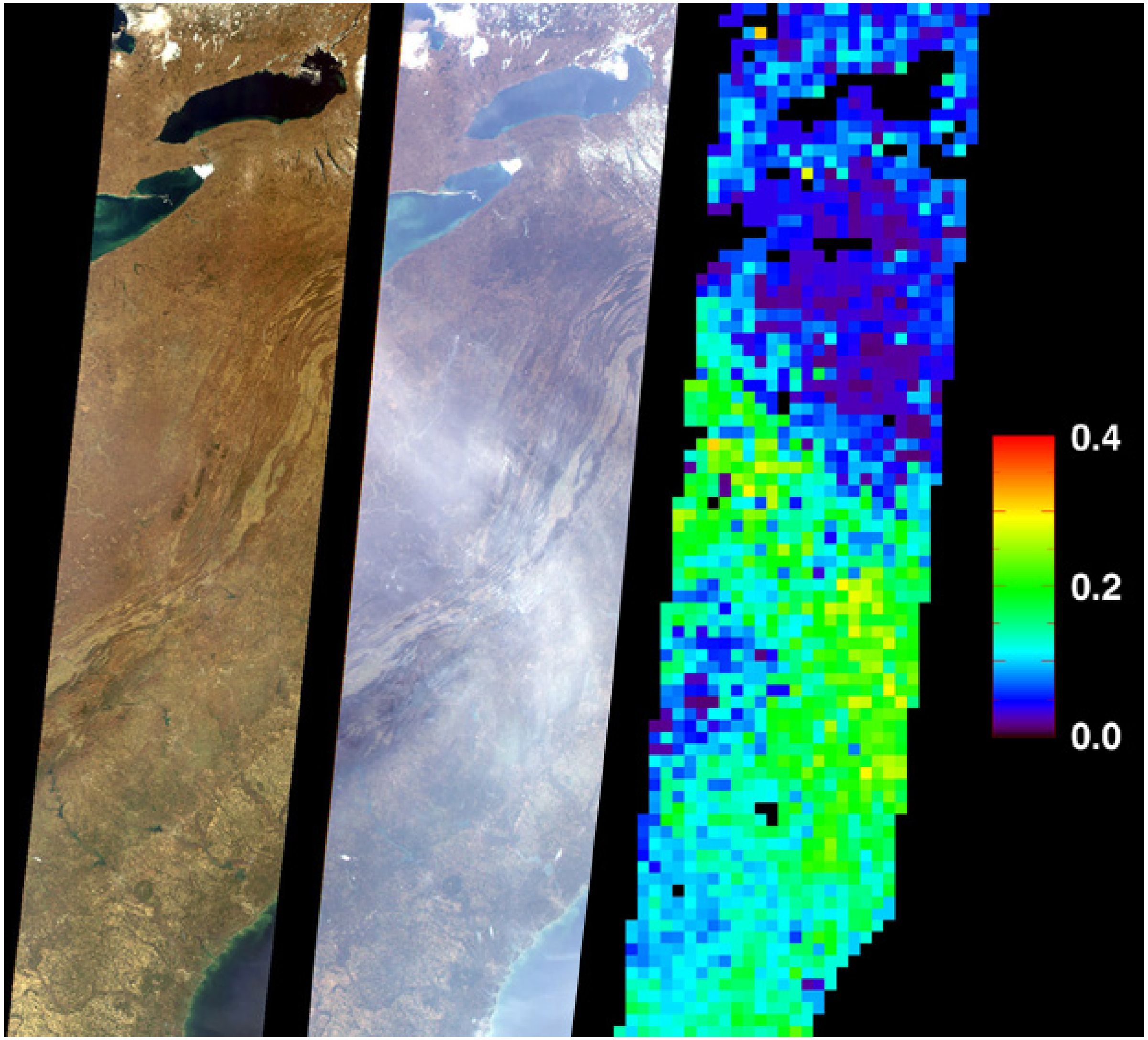

Thin haze over land is difficult to detect in the nadir view due to the brightness of the land surface

The longer atmospheric path length enhances the haze path radiance

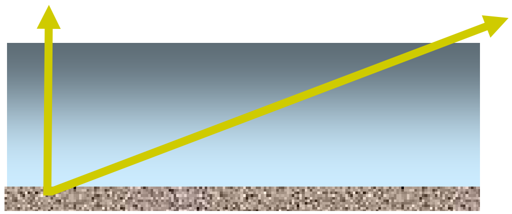

Avoiding sunglint

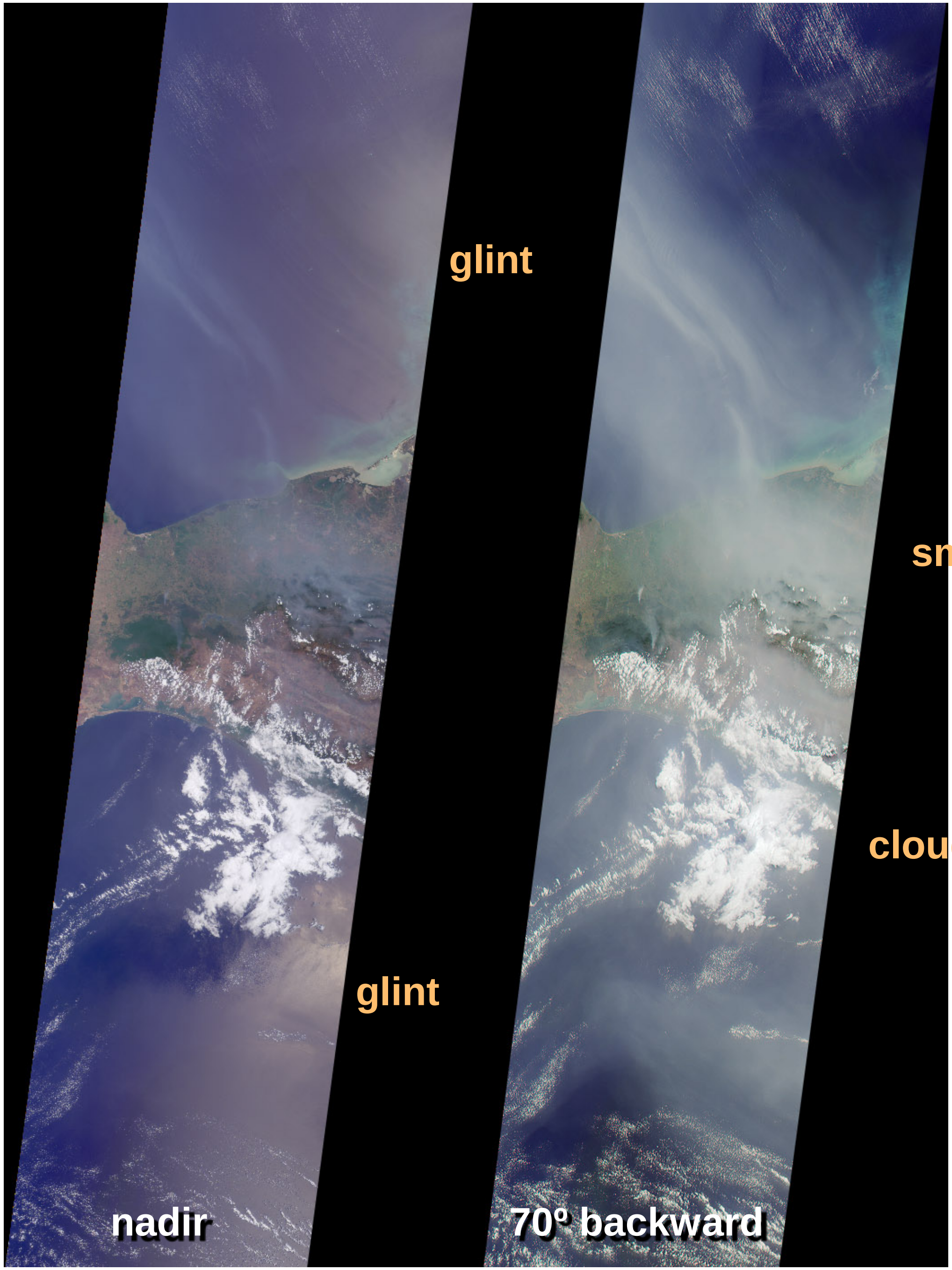

Sunglint over water invalidates the assumption of a dark surface, and multiple cameras provide the flexibility to avoid this

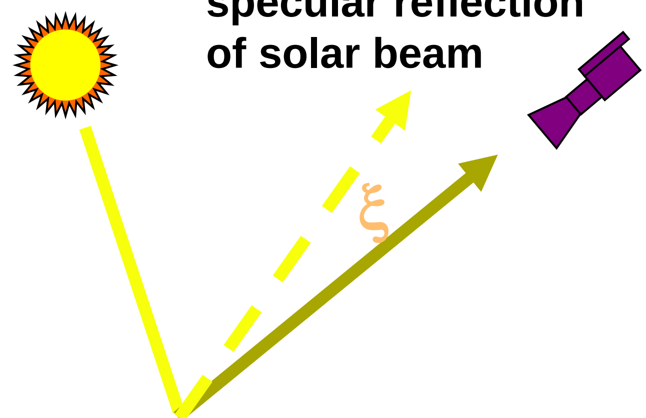

MISR aerosol retrievals require glitter avoidance of at least 40º

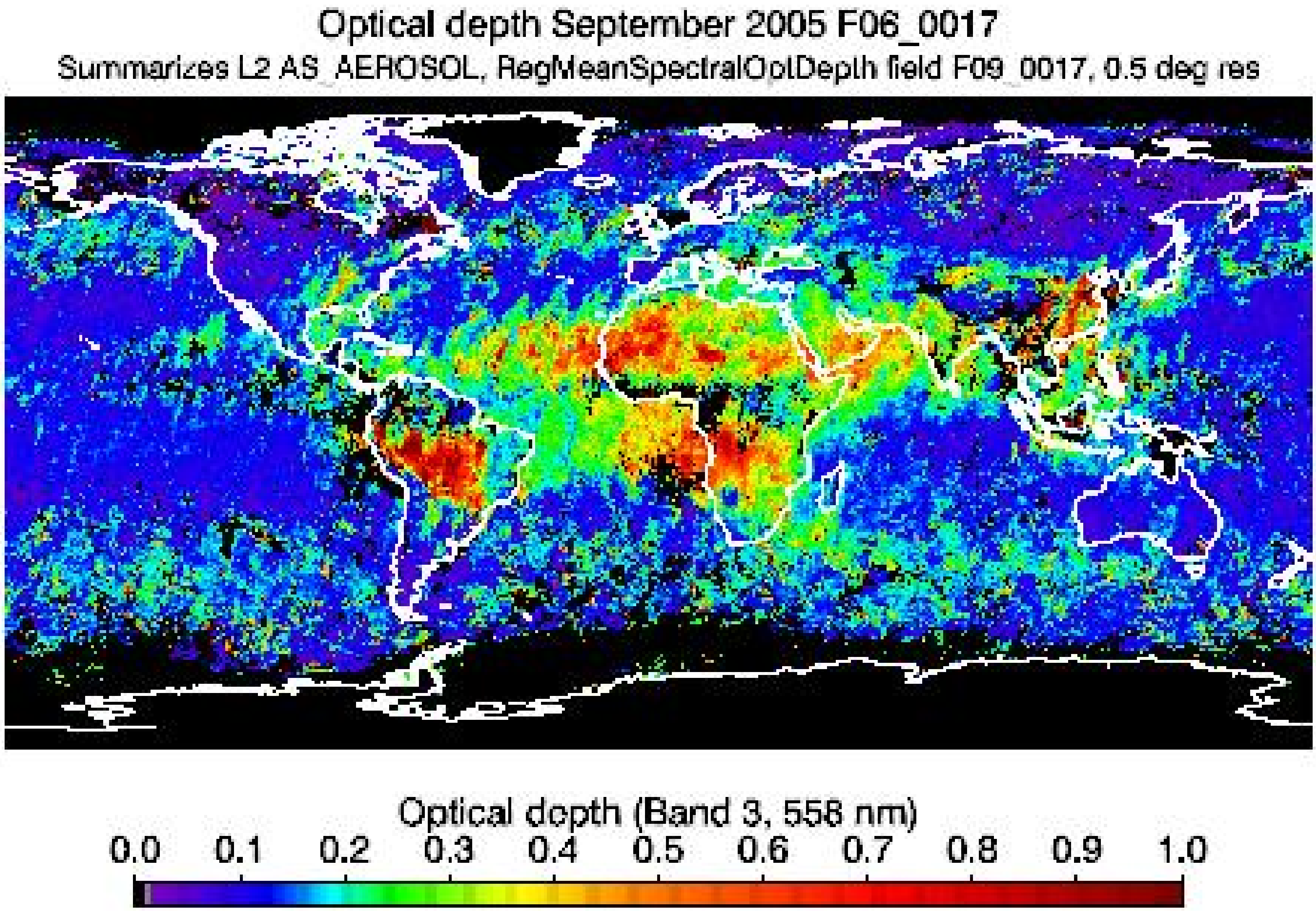
Optical depth September 2005 F06_0017
Summarizes L2 AS_AEROSOL, RegMeanSpectralOptDepth field F09_0017, 0.5 deg res
Optical depth (Band 3, 558 nm)
0.0
0.1
0.2
0.3
0.4
0.5
0.6
0.7
0.8
0.9
1.0

Radiance and Polarization Measurements from POLDER

Western Europe
March 10, 1997

R = 0.865 μm
G = 0.670 μm
B = 0.443 μm

Radiance

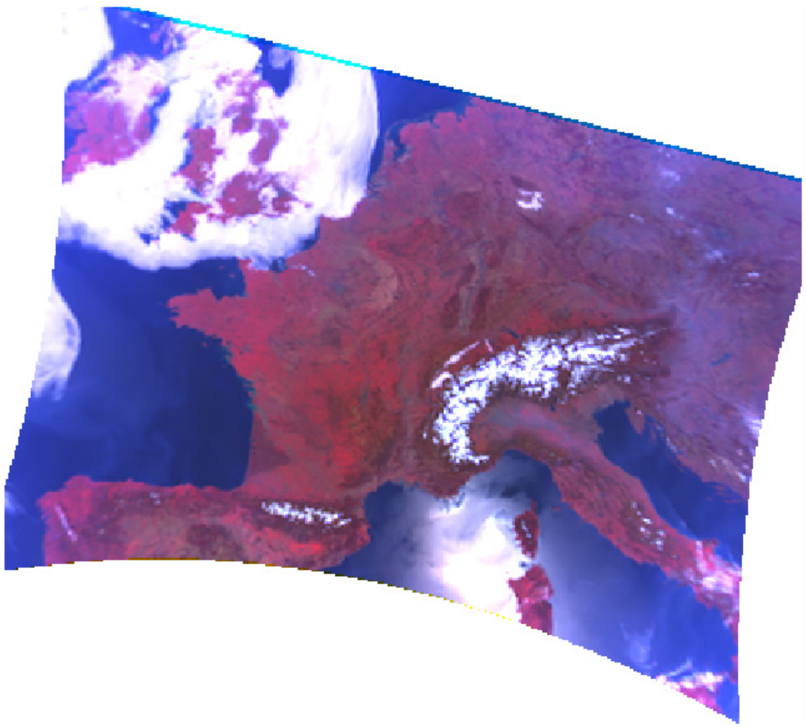

Polarization

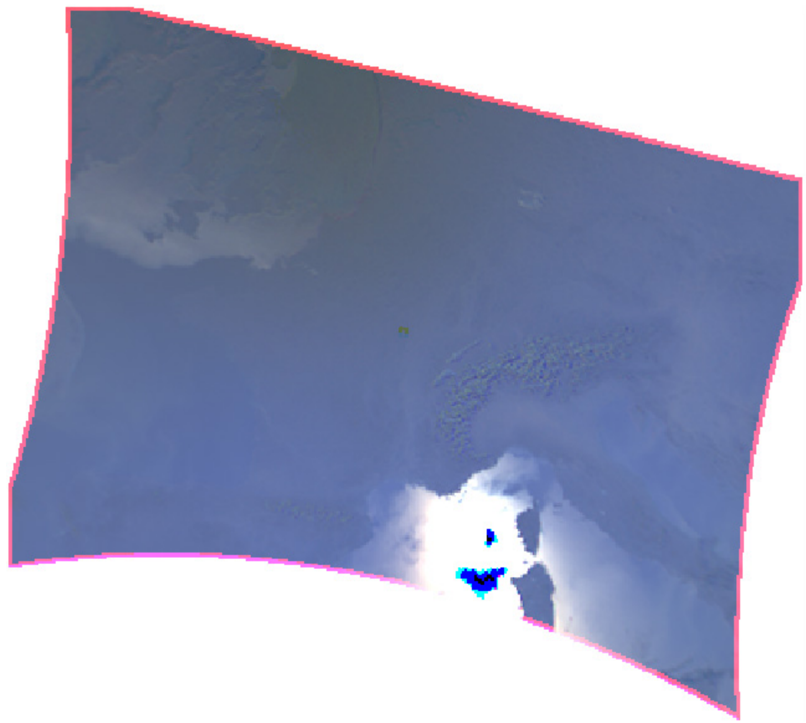

Notice the land

Aerosol Optical Thickness

POLDER
April 1997

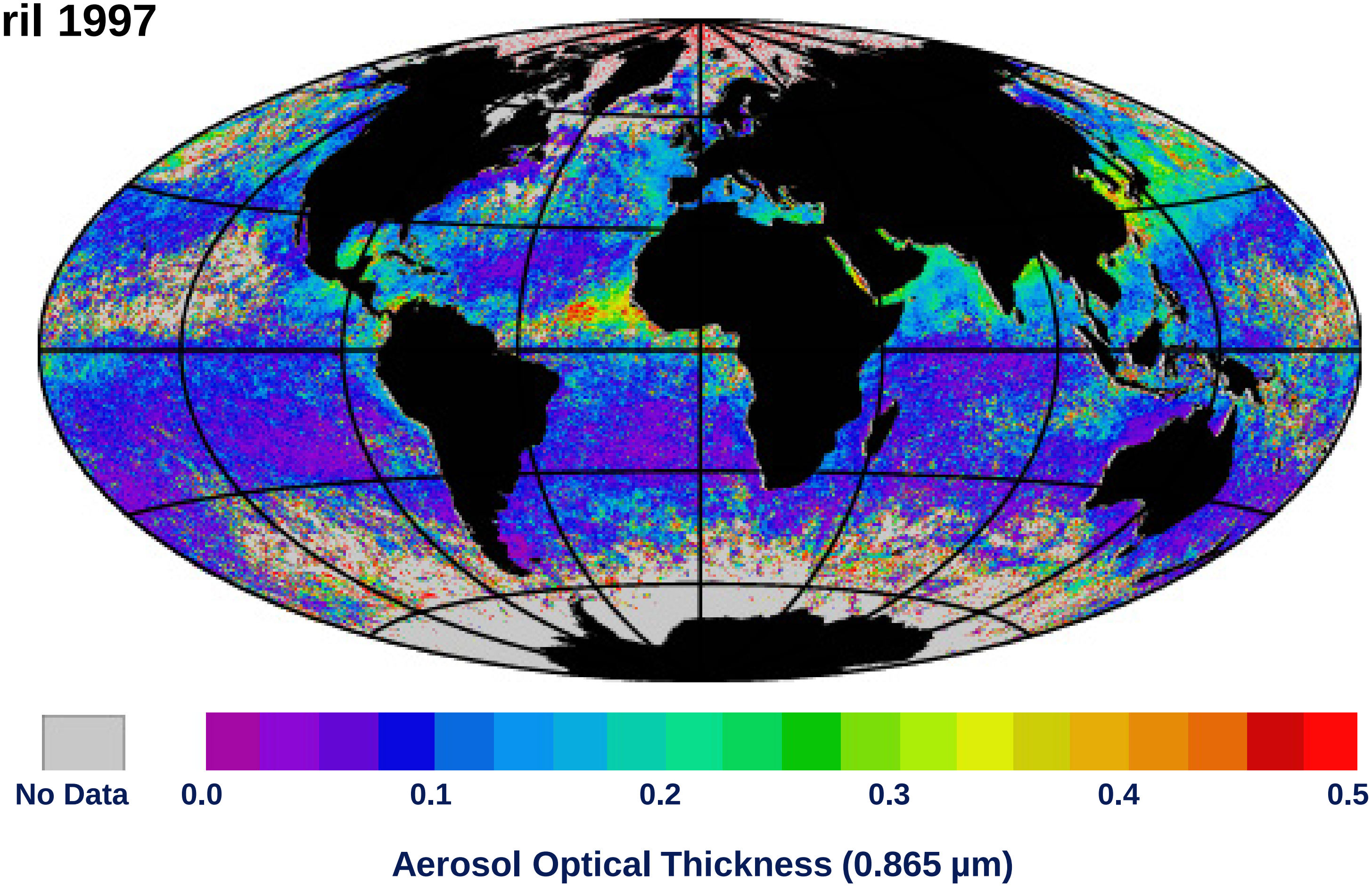

Ångström Exponent

POLDER
April 1997

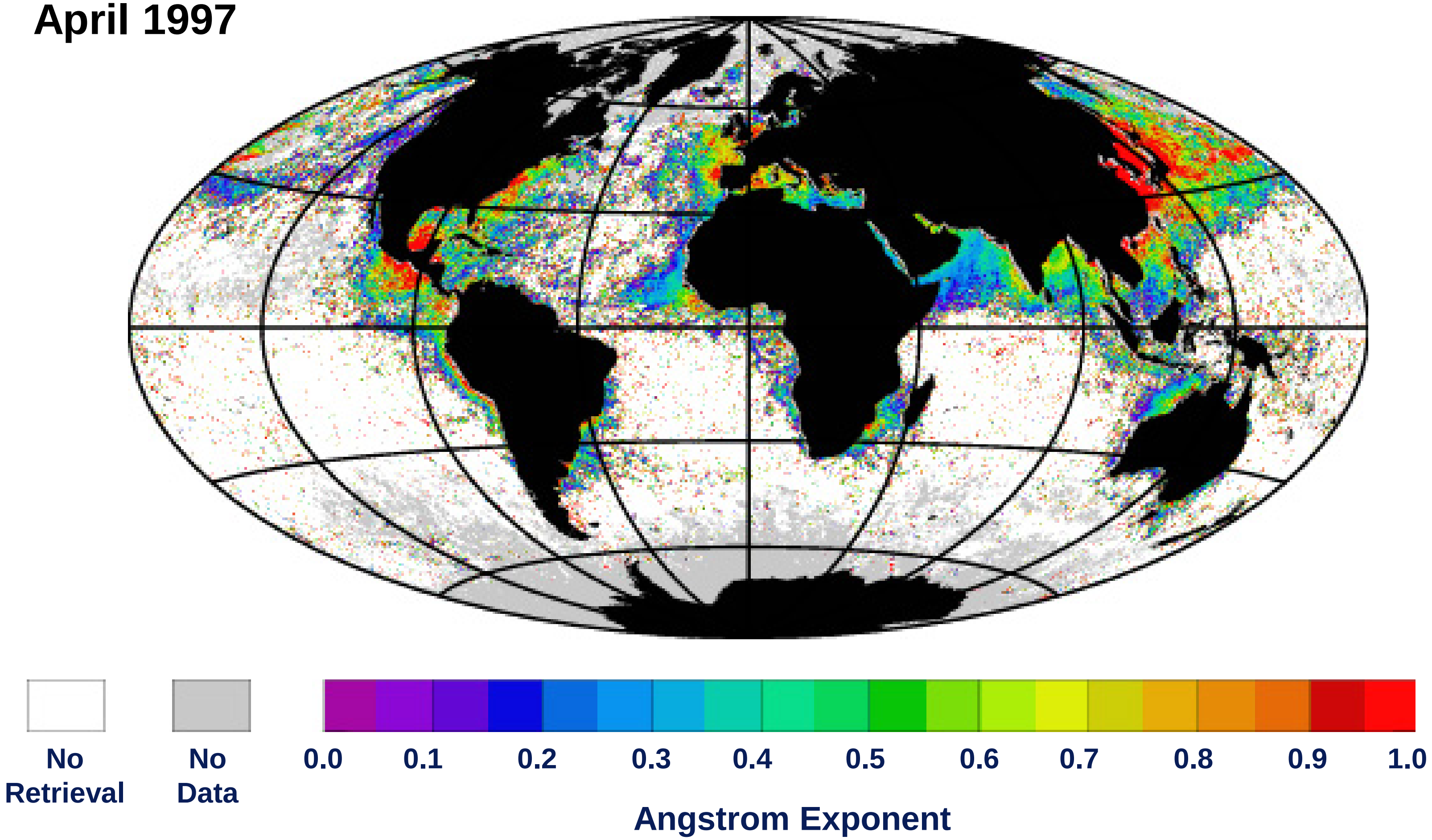

SATELLITE MEASUREMENTS OF AEROSOL MASS AND TRANSPORT

Atmospheric Environment, 1984.

ROBERT S. FRASER

Laboratory for Atmospheric Sciences, NASA/Goddard Space Flight Center, Greenbelt, MD 20771, U.S.A.

YORAM J. KAUFMAN

University of Maryland in collaboration with Goddard Laboratory for Atmospheric Sciences, NASA/Goddard Space Flight Center, Greenbelt, MD 20771, U.S.A.

and

R. L. MAHONEY

Science Systems and Applications, Inc. 10210 Greenbelt Road, Seabrook, MD 20706, U.S.A.

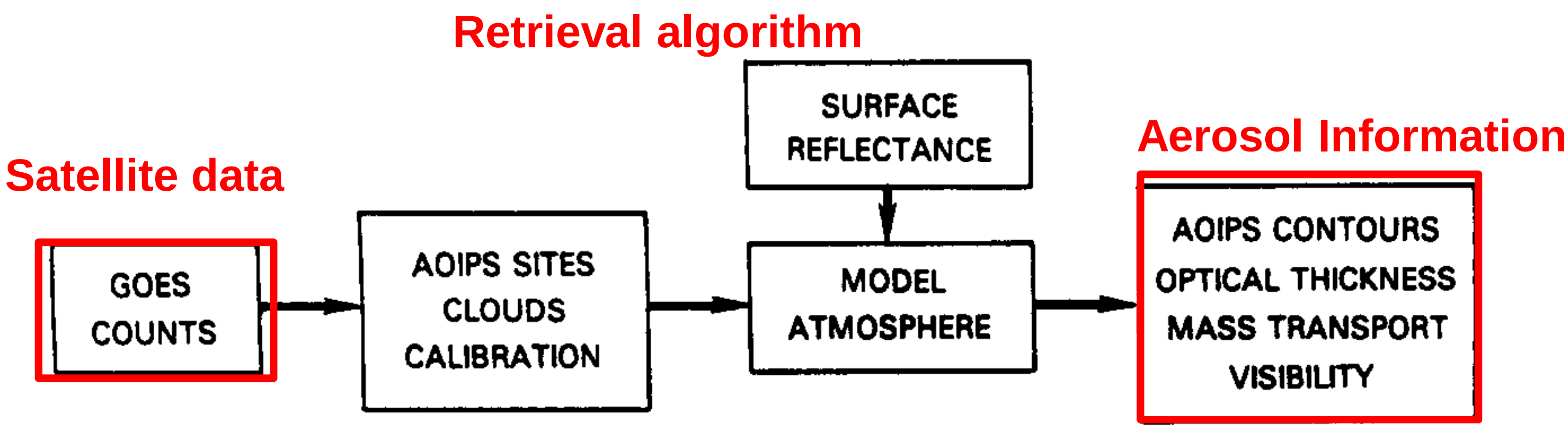

Fig. 3. Algorithm for deriving aerosol properties from satellite observations.

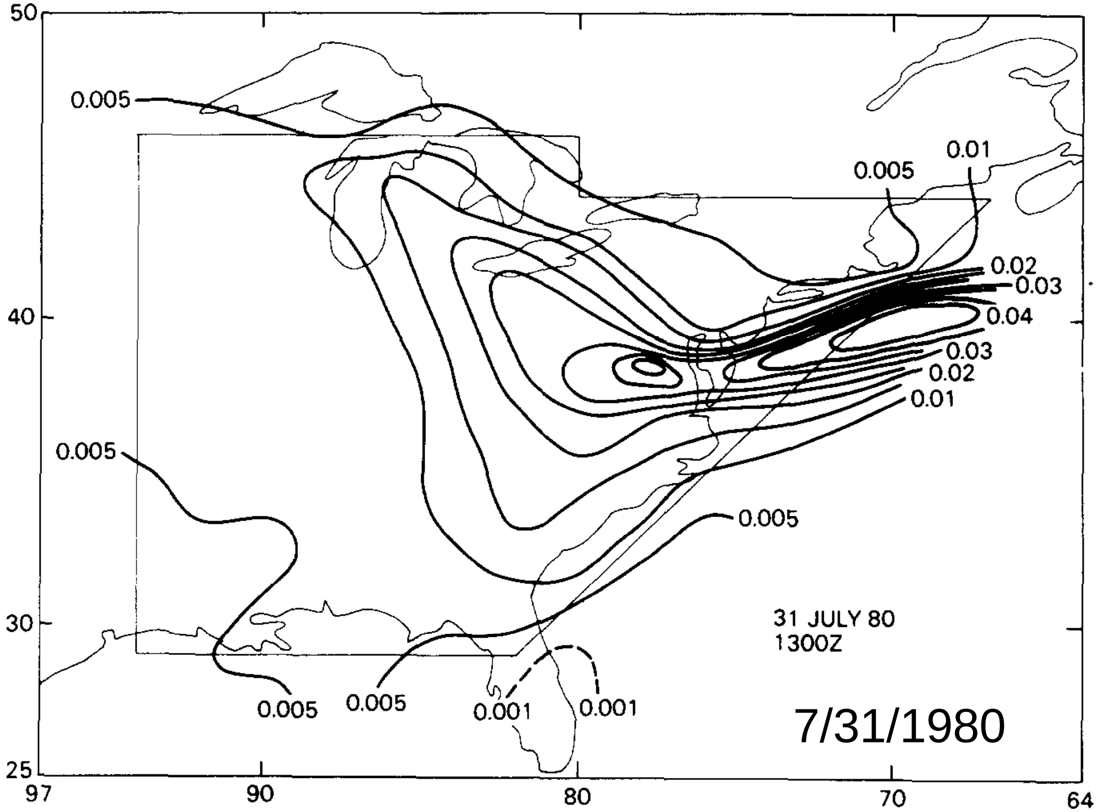

Atmospheric loading of particulate sulfur (gm^{-2}) on 31 July 1980.

Derived from GOES visible reflectance are

- **Aerosol optical thickness (AOT)/depth (AOD)**
- **Columnar amount of sulfur**

Table 1. Comparison of columnar masses of sulfur derived from ground-based and satellite observations. The satellite observations were made at 1300 GMT on 31 July 1980

1 Place	2 Latitude (deg. N)	3 Longitude (deg. W)	4 Particulate sulfate mass ($\mu g\ m^{-3}$)	5 Columnar sulfur mass ($g\ m^{-2}$)	6 Reference	7 Satellite sulfur mass ($g\ m^{-2}$)	8 Ratio columns 7 and 5
Virginia	38.7	78.3	38	0.018	Ferman *et al.* (1981)	0.040	2.3
Virginia	38.7	78.3	38	0.018	Stevens *et al.* (1984)	0.040	2.3
Near Baltimore	39.3	76.4	24	0.014	Tichler *et al.* (1981)	0.017	1.2

Satellite Remote Sensing of Aerosol Transport

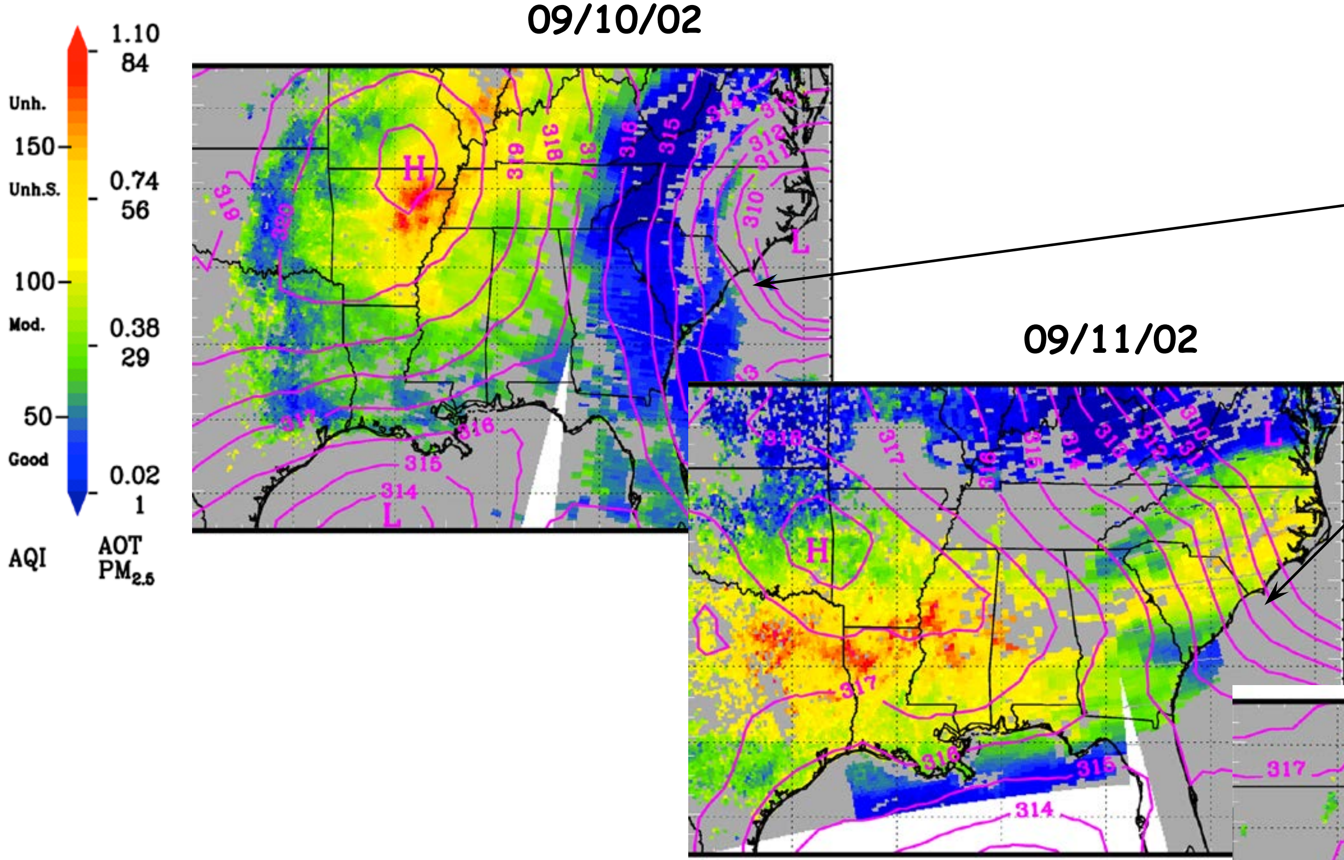

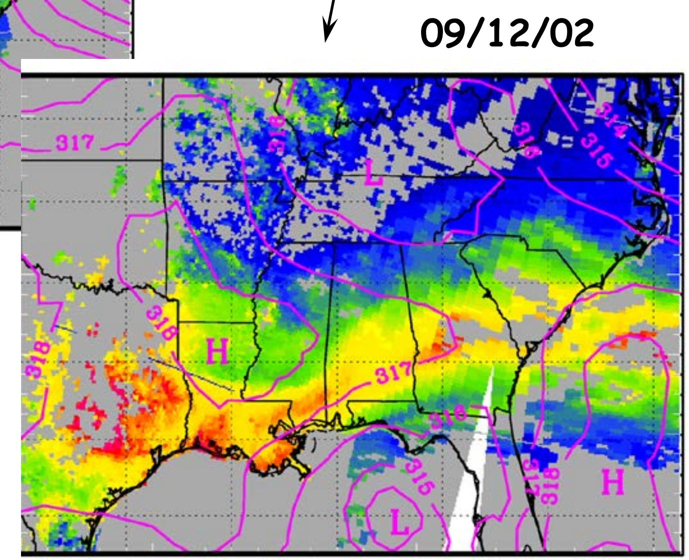

MODIS Aerosol Optical Thickness &
700mb Geopotential Height

PM2.5 = A*AOD + B

Wang & Christopher, 2003;
Citation: ~360

Past studies on AOD vs. surface PM concentration

(from Hoff and Christopher, 2009, JAWMA)

2003

Author	Sensor	Date	Region	Number of Ground Monitors	$PM_{2.5}/PM_{10}$	Linear Regression	R
Wang[154]	MODIS (Terra)	2002	Alabama	7	$PM_{2.5}$ (24 hr)[a]	$77.0\tau - 0.23$	0.67
	MODIS (Aqua)	2002	Alabama	7	$PM_{2.5}$ (24 hr)[a]	$68.6\tau + 1.93$	0.76
	Average	2002	Alabama	7	$PM_{2.5}$ (24 hr)[a]	$72.3\tau + 0.85$	0.98
Chu[153]	MODIS	August–October 2000	Italy	1	PM_{10}	$54.7\tau + 8.0$	0.82
Engel-Cox[161]	MODIS	April–September 2002	United States	1338	$PM_{2.5}$	$22.6\tau + 6.4$	0.4
					$PM_{2.5}$ (24 hr)	$18.7\tau + 7.5$	0.43
Liu[208]	MISR	2003	St. Louis	22	$PM_{2.5}$	NA	0.8
Engel-Cox[163]	MODIS	July 1 to August 30, 2004	Baltimore	4	$PM_{2.5}$	$31.1\tau + 5.2$	0.65
					$PM_{2.5}$ (<PBL)	$48.5\tau + 6.2$	0.65
					$PM_{2.5}$ (24 hr)	$25.3\tau + 11.1$	0.57
					$PM_{2.5}$ (24 hr < PBL)	$64.8\tau + 1.76$	0.76
Liu[169]	MISR	2001	Eastern United States	346	$PM_{2.5}$		–
Al-Saadi[164]	MODIS	Review	United States		$PM_{2.5}$	62.0τ	NA
Gupta[171]	MODIS	2002 and July–November 2003	Global cities	26	PM_{10}[a]	$141.0\ \tau$	0.96
Koelemeijer[152]	MODIS	2003	Europe	88 ($PM_{2.5}$)	$PM_{2.5}$[a]	NA	0.63
					PM_{10}[a]	$214.0\tau - 42.3$	0.58
Kacenelenbogen[118]	POLDER	April–October 2003	France	28	$PM_{2.5}$	$26.6\tau + 13.2$	0.7
Gupta[173]	MODIS	February 2000 to December 2005	Southeastern United States	38	$PM_{2.5}$	$29.4\tau + 8.8$	0.62
					$PM_{2.5}$ (24 hr)	$27.5\tau + 15.8$	0.52
Hutchison[158]	MODIS	August–November 2003 and 2004	Texas	28	$PM_{2.5}$ (August)[a]	$68.8\tau - 39.9$	0.47
					$PM_{2.5}$ (September)[a]	$59.7\tau - 17.2$	0.98
Paciorek[177]	GOES-12	2004	United States	Not given	$PM_{2.5}$ (24 hr)	NA	0.5
					$PM_{2.5}$ (yearly)	NA	0.75
An[179]	MODIS	April 3–7, 2005	Beijing	6	PM_{10}[a]	$21.7\tau + 6.1$	0.92
					$PM_{2.5}$[a]	$31.1\tau + 5.1$	0.92
					$PM_{2.5}$	$120\tau + 5.1$	0.72

2009

multivariate regression, Kriging, neutral network, etc…

AOD sometimes is a good indicator of surface PM

~200 sites over continental U.S.

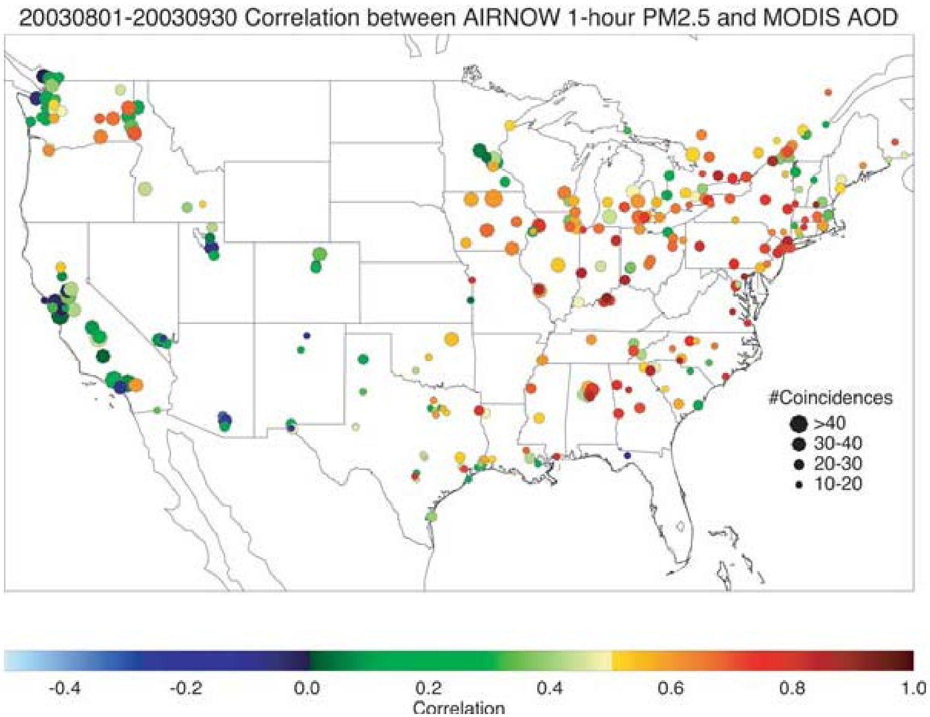

PM vs AOT linear correlation coefficient

Engel-Cox et al., 2004, JAWMA.

$$\tau = f(rh) \times Q_{dext}(0) \times m_{daer}(0) \times H_{eff} \quad (1)$$

$Q_{dext}(0)$ is the mass extinction efficiency (m^2g^{-1}) of dry particles at the surface,

$m_{daer}(0)$ is the mass concentration (gm^{-3}) of dry aerosol particles at the surface,

f(rh) is a hygroscopic growth factor that considers the change of aerosol extinction efficiencies due to the solubility (hygroscopicity) of aerosols.

H_{eff} is effective scale height (dependent on the shape of aerosol extinction vertical profile)

Integrating satellite & model

Simple regression **With inputs of models**

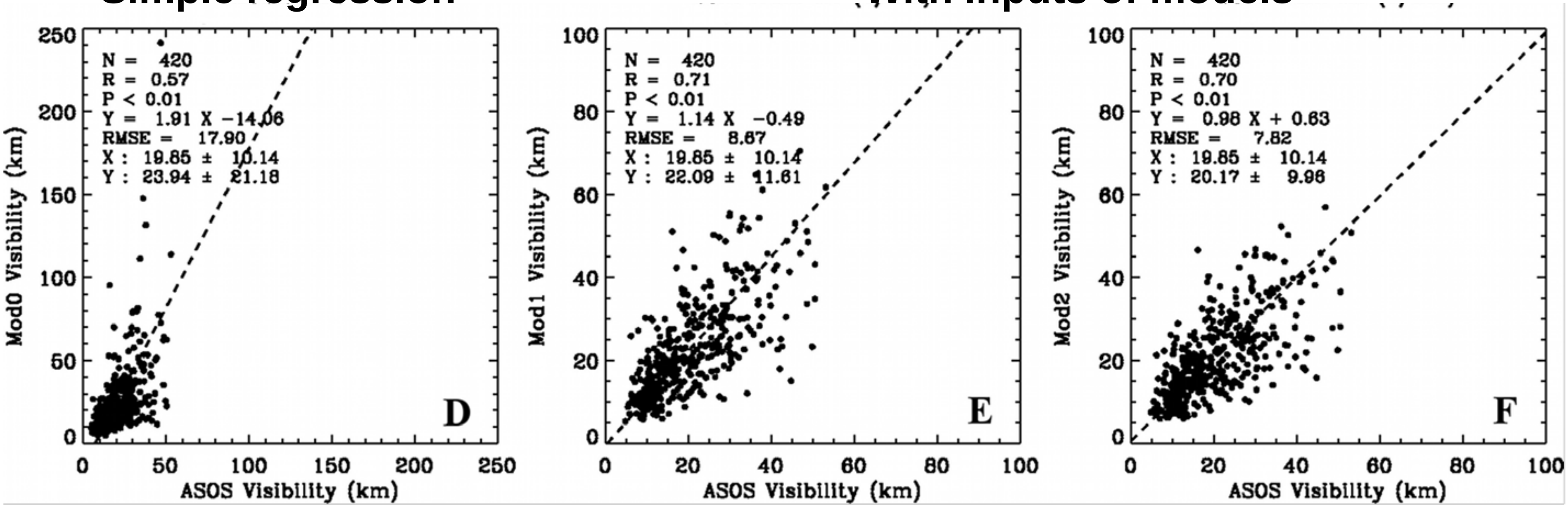

Mapping visibility from space

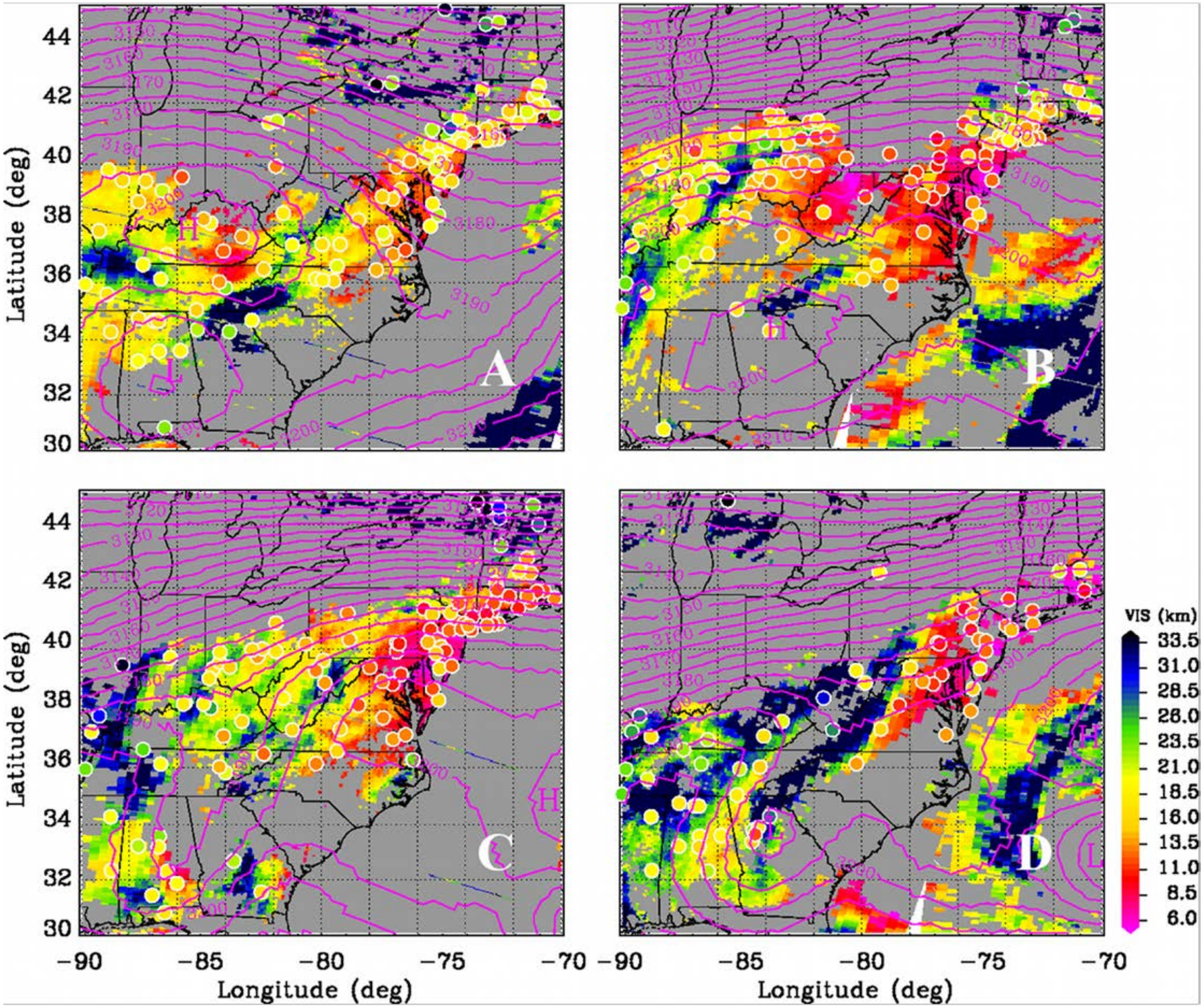

11 - 14 August 2005.

Use MODIS + chemistry transport adjoint model to constrain emissions

Prior emission from ground report

Posterior Emission from MODIS radiance

SO_2

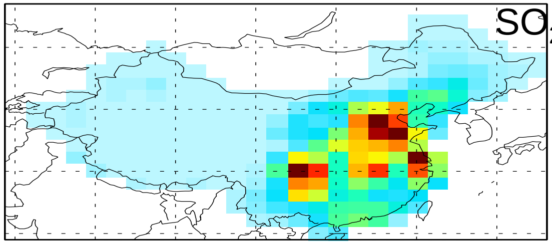

N/A

Xu, Wang, Henze et al., JGR, 2014

NO_2

N/A

BC

N/A

Dust

N/A

Using satellite data, we found a reduction of SO_2 emission in 2008 as compared to 2006 because of preparation for 2008 Olympics.

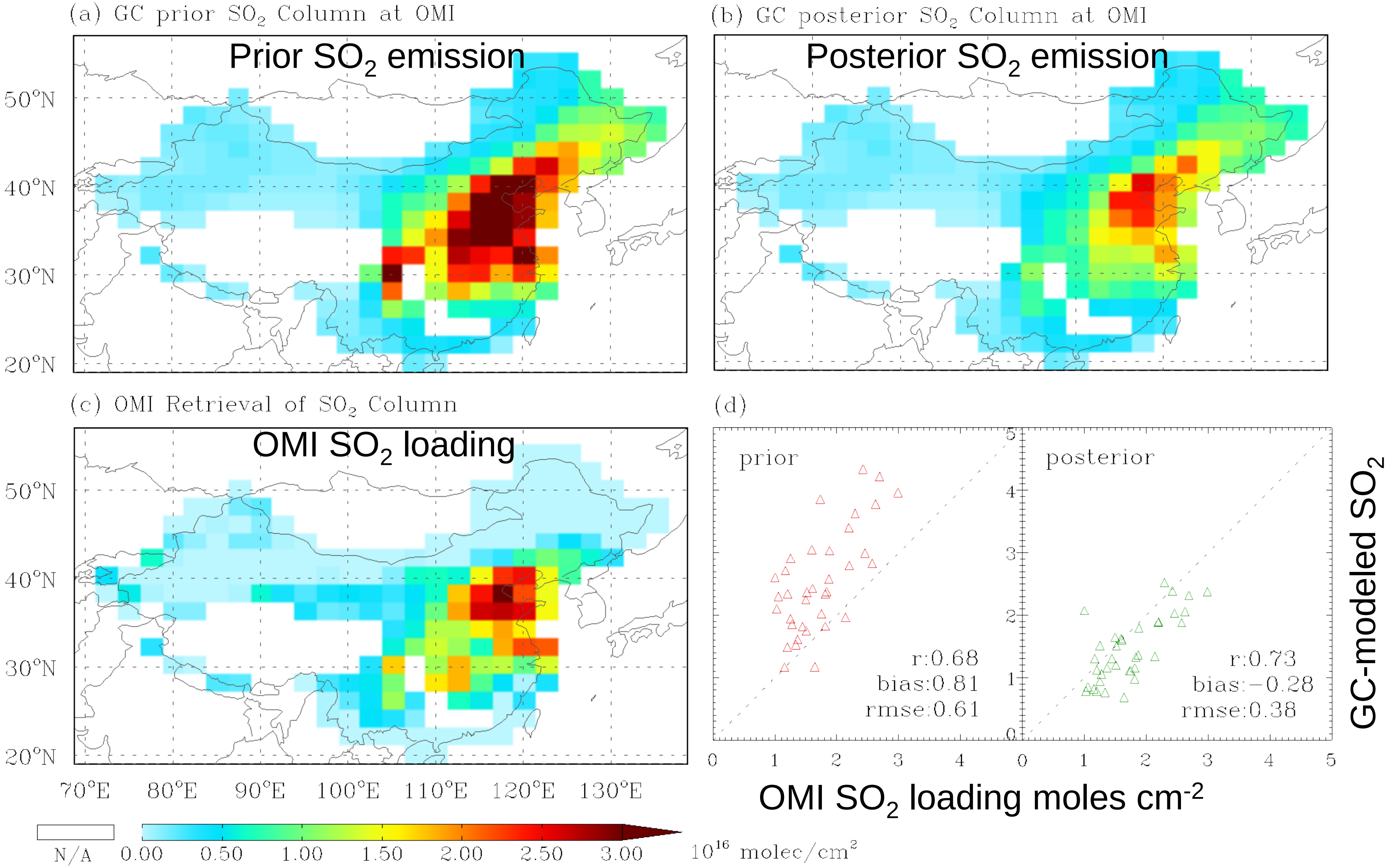

We also found a reduction of NO_2 emission in 2008.

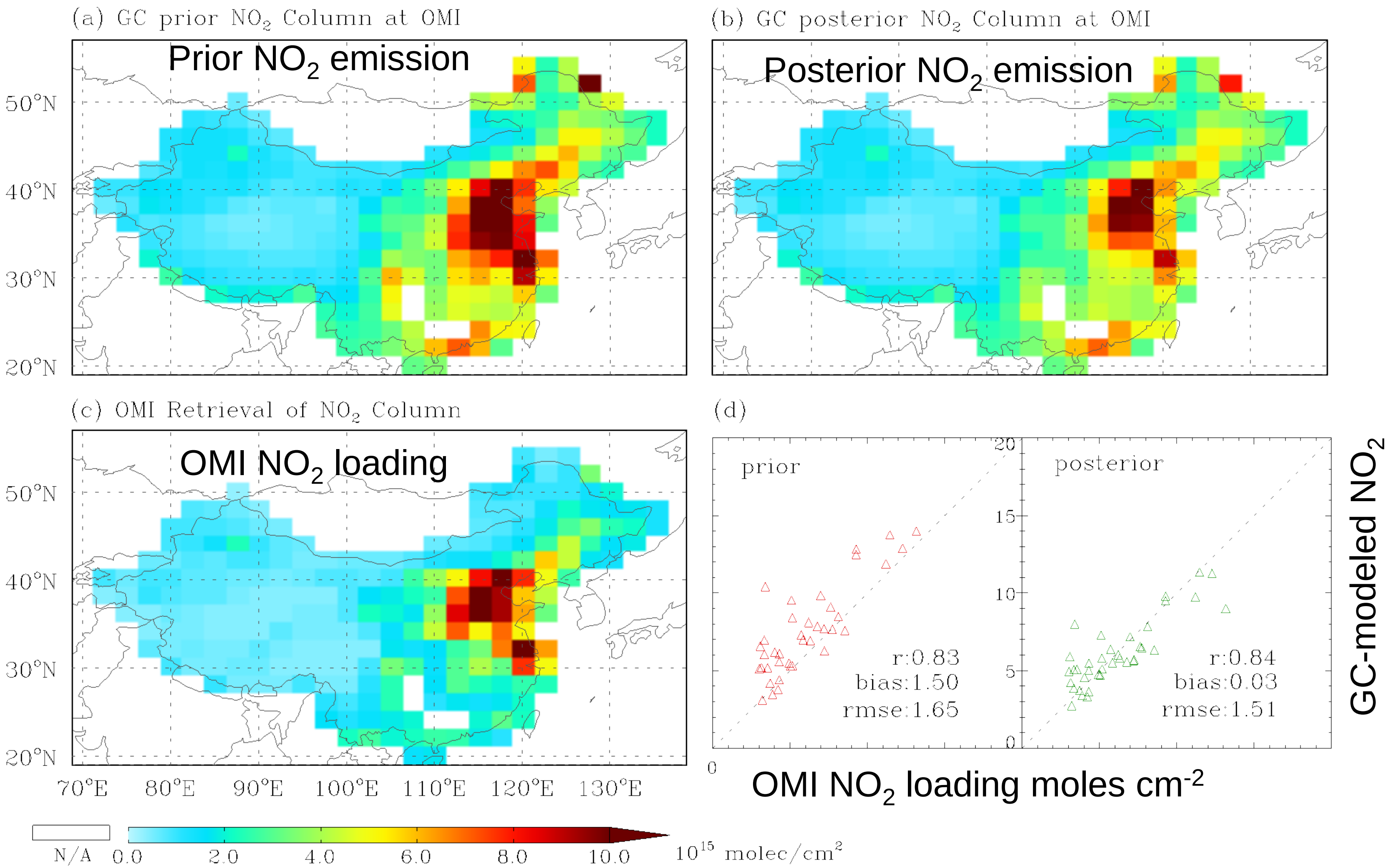

Validation results over the ground station

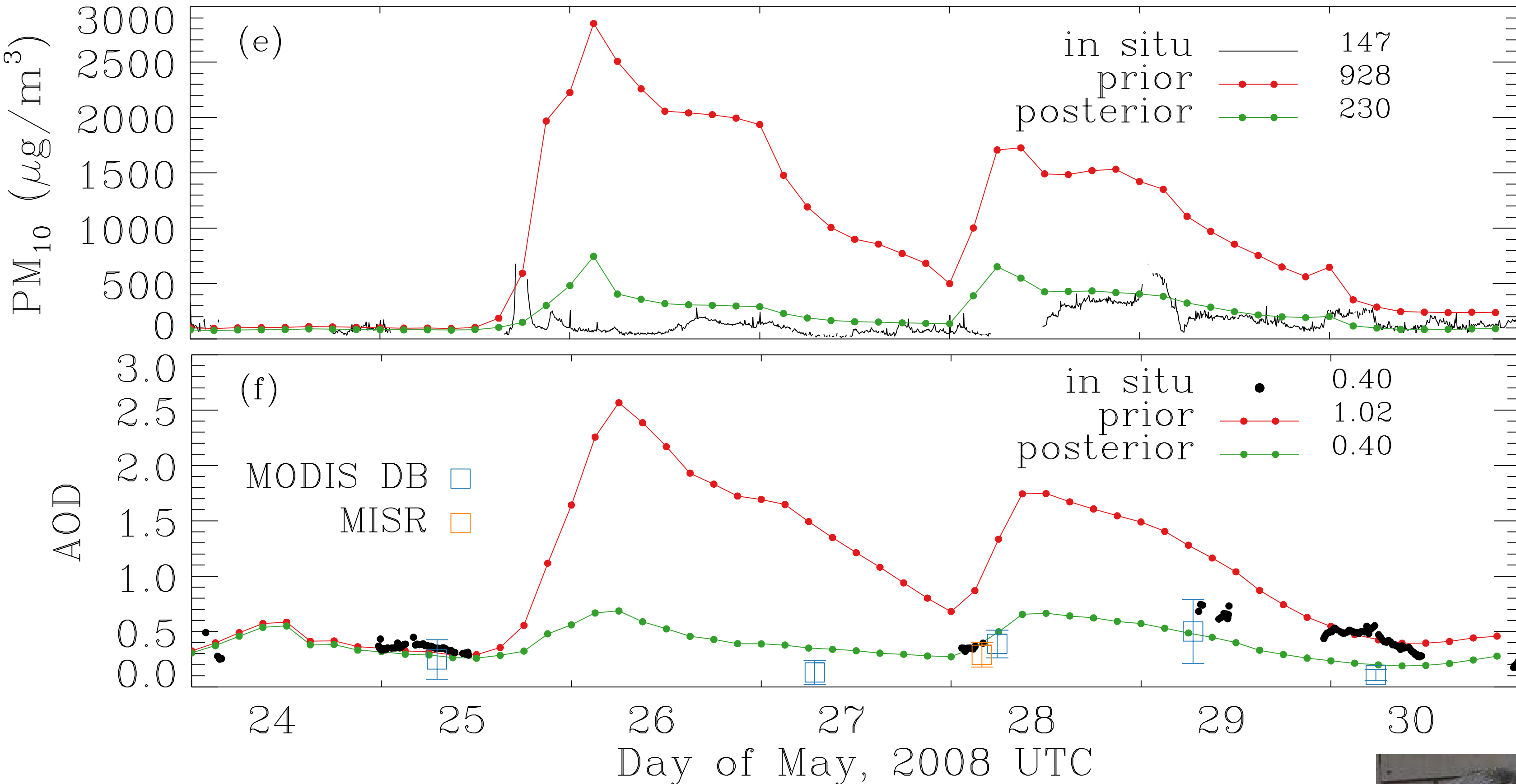

In situ data measured at Zhangye (39.08 N, 100.3 E) is provided by Qiang Ji, Si-Chee Tsay, and others in a DOE project in 2008.

Xiaoguang XU et al., JGR; Wang et al., JGR.

Looking ahead

- **Algorithm with more constraints from temporal and spatial continuity and smoothness (Dubovik et al., 2014; Lyapustin et al., 2014)**
- **Using O2 A + B + polarization to retrieve aerosol height (Wang et al., 2014; Hou et al., 2016)**
- **Combine MODIS + OMI (Torres et al., 2015)**
- **Combine observation with models for air quality applications (emissions, surface PM, etc.).**
- **Geostationary + UV-Vis hyperspectral (TEMPO; Chance et al.)**
- **Multiple angle + multiple wavelength + polarization (MAIA; Diner et al.)**




MAIA

Associating airborne particle types with adverse health outcomes

Multi-Angle Imager for Aerosols (MAIA)



The following slides are provided by MAIA PI:
David Diner
JPL

MAIA objective

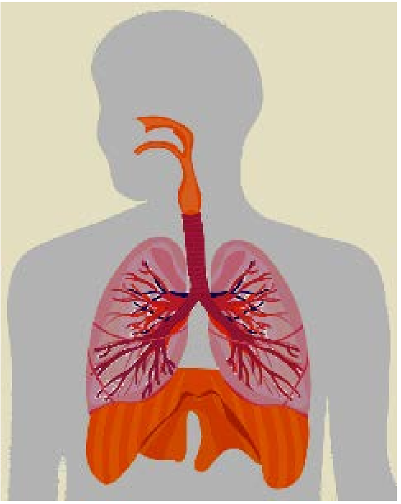

Coarse particles irritate and inflame our respiratory systems.

Fine particles penetrate deep into our lungs and carry toxins into our bloodstreams.

Airborne **particulate matter (PM)** is a well-known cause of cardiovascular and respiratory diseases, heart attacks, low birth weight, lung cancer, and premature death.

But the relative toxicity of specific **PM types** is poorly understood.

MAIA is designed to fill this gap in our understanding and enable more cost-effective pollution controls and improved health outcomes.

MAIA investigation approach

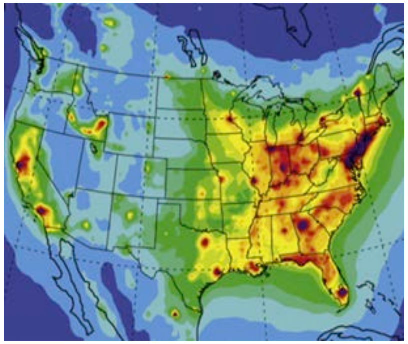

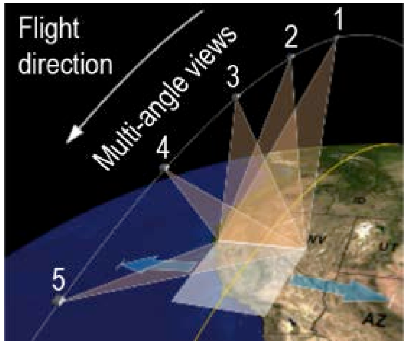

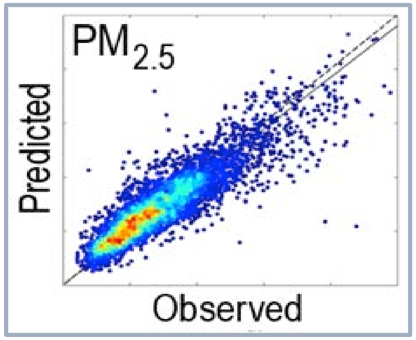

The WRF-Chem chemical transport model (CTM) provides initial estimates of the abundances of different aerosol types, along with their vertical distributions.

The MAIA instrument uses multi-angle and multispectral radiometry and polarimetry to eliminate CTM biases and retrieve fractional aerosol optical depths of different particle types.

Geostatistical models (GSMs) derived from collocated surface and MAIA measurements relate fractional aerosol optical depths to near-surface concen-trations of major PM constituents.

Geocoded birth, death, and hospital records and epidemiological methodologies are used to associate PM exposure with adverse health outcomes.

MAIA cameras are mounted on a 2-axis gimbal for targeted science operations and calibration

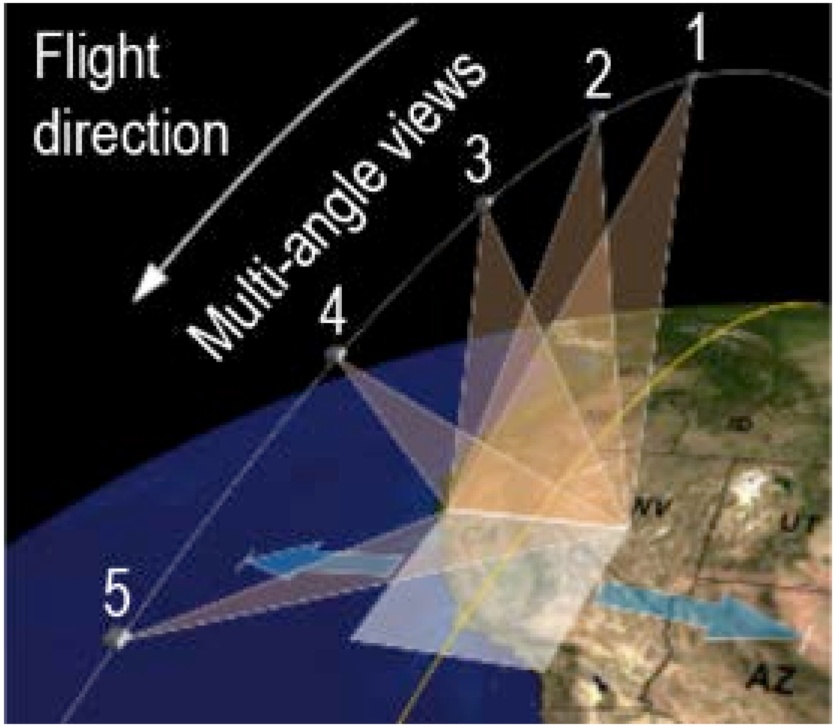

Along-track axis provides step-and-stare multiangle imagery (±60º at instrument)

Cross-track axis proves axis to targets off the sub-satellite track (±45º at instrument)

Swath width and spatial resolution

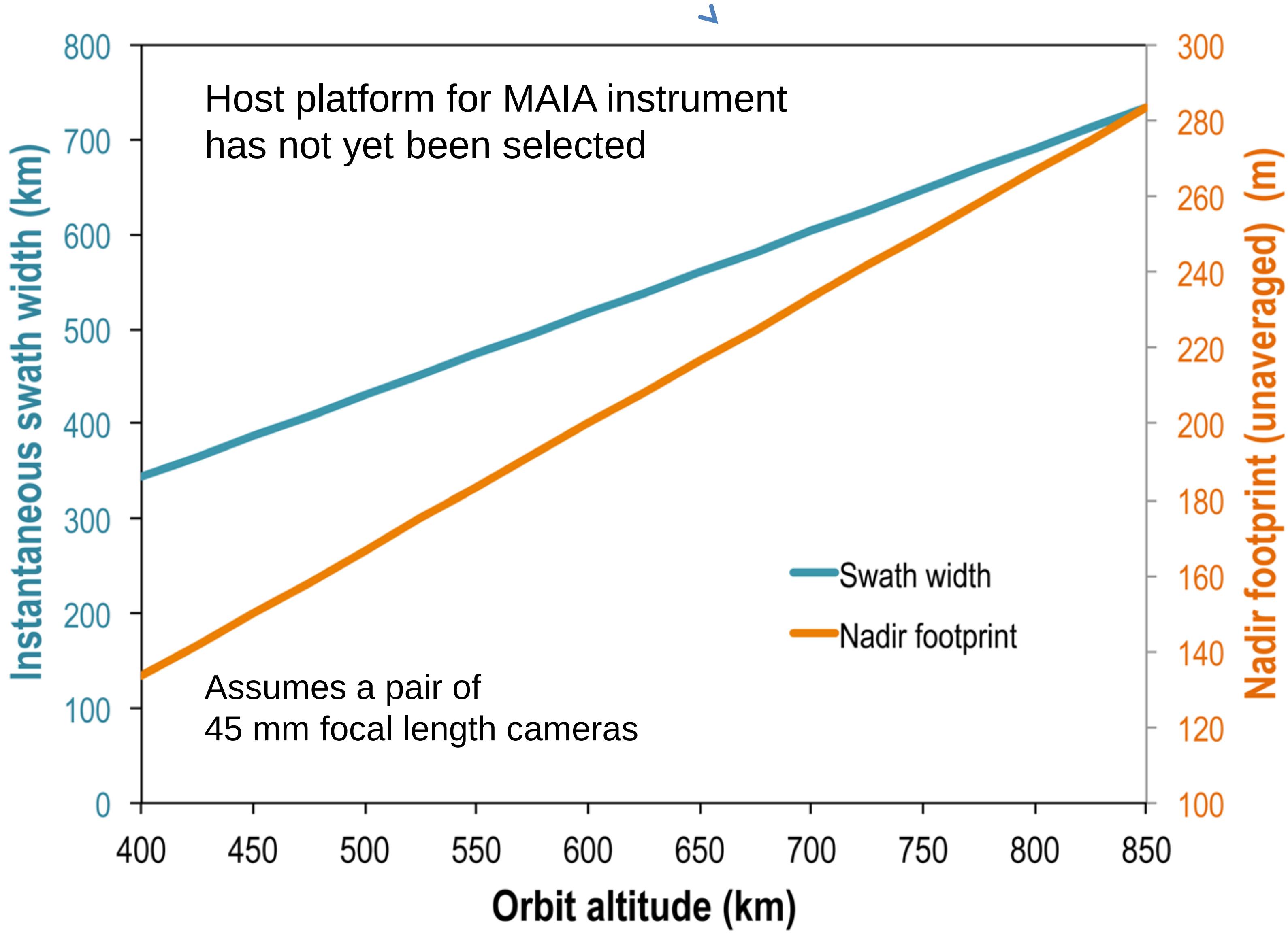

MAIA spectral bands

Band center (nm)	FWHM (nm)
367	57
386	56
445	57
543	37
645	67
751	4.3
763	4.8
862	48
945	34
1620	141
1888	98
2185	170

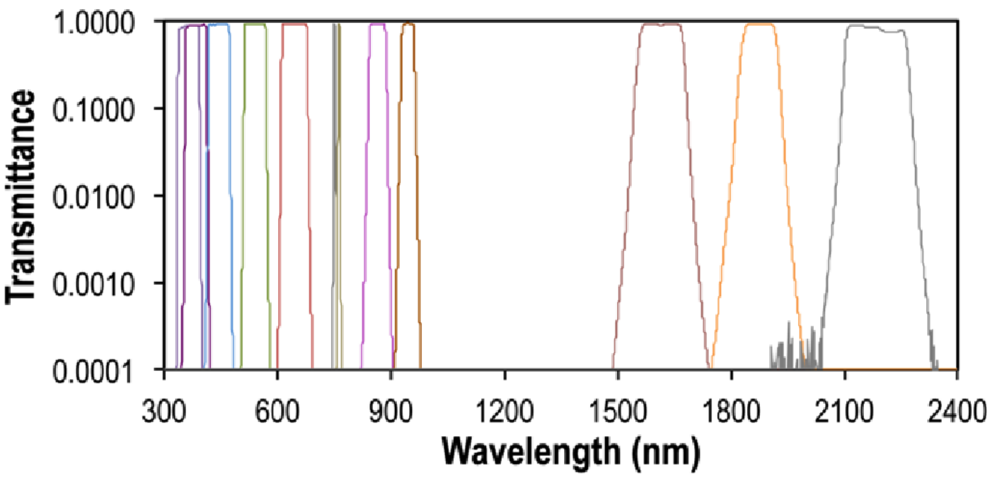

Radiometric Polarimetric

VNIR and shortwave infrared (SWIR) bands help discriminate particle size. 1888 nm provides cirrus screening

UV bands are sensitive to absorption by iron and aluminum oxides in dust particles, nitrated aromatic and polycyclic aromatic hydrocarbons in organic aerosols, and soot

Multiangle intensity and polarization helps discriminate particle size and shape, and compositional proxies like refractive index

Summary & look ahead

- So far, AOD is still the most reliable variable we retrieve for aerosols;
- Aerosol single scattering abledo, height, size, etc., are coming along;
- Since surface PM is of high concern in AQ, vertical profile of aerosols, for the most, has to come from models – data assimilation .

Future Directions

- Geostationary + UV-Vis hyperspectral (TEMPO; Chance et al.)
- Multiple angle + multiple wavelength + polarization (MAIA; Diner et al.)
- Algorithm with more constraints from temporal and spatial continuity and smoothness (Dubovik et al., 2014; Lyapustin et al., 2014)
- Using O2 A + B + polarization to retrieve aerosol height (Wang et al., 2014; Hou et al., 2016)
- Combine MODIS + OMI (Torres et al., 2015)
- Combine observation with models for air quality applications (emissions, surface PM, etc.).

Outlook

An exciting field, with more discoveries & applications to come !

Thank you !

Aerosol observation from space by solar backscatter

(Aerosol ≡ Particulate Matter)

Easy to do qualitatively…

California fire plumes

Pollution off U.S. east coast

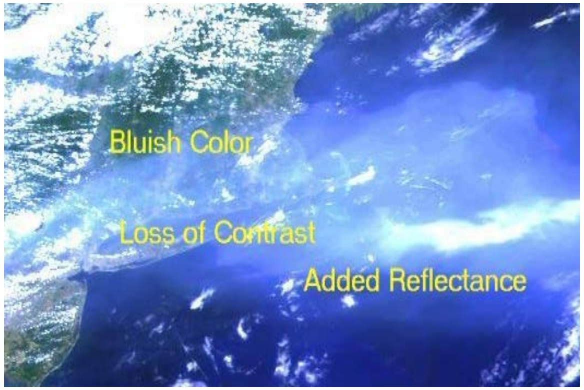

Dust off West Africa

…but diifcult quantitatively! Weak spectral structure complicates separation from surface backscatter

Challenges: Aerosol optical property

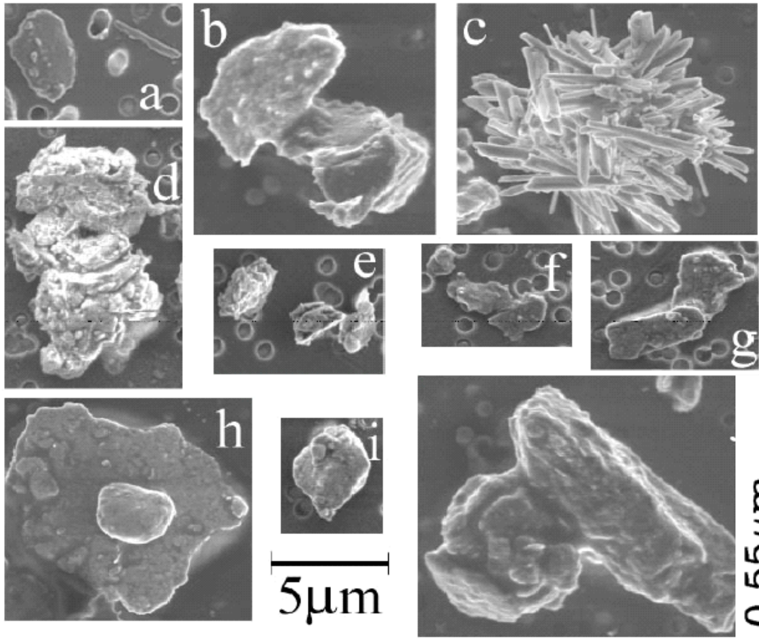

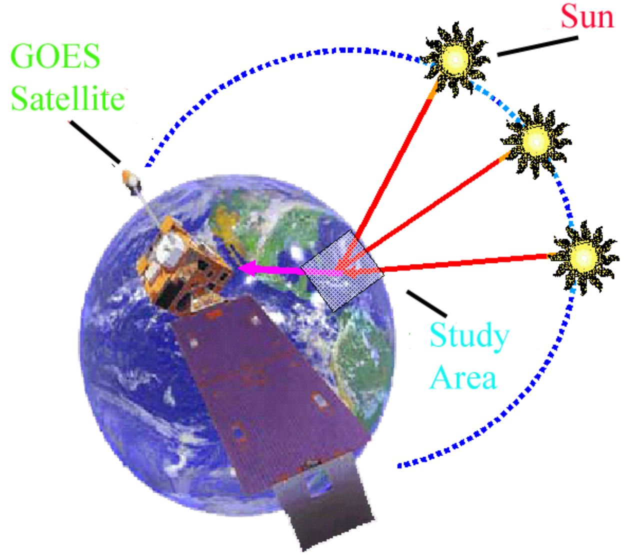

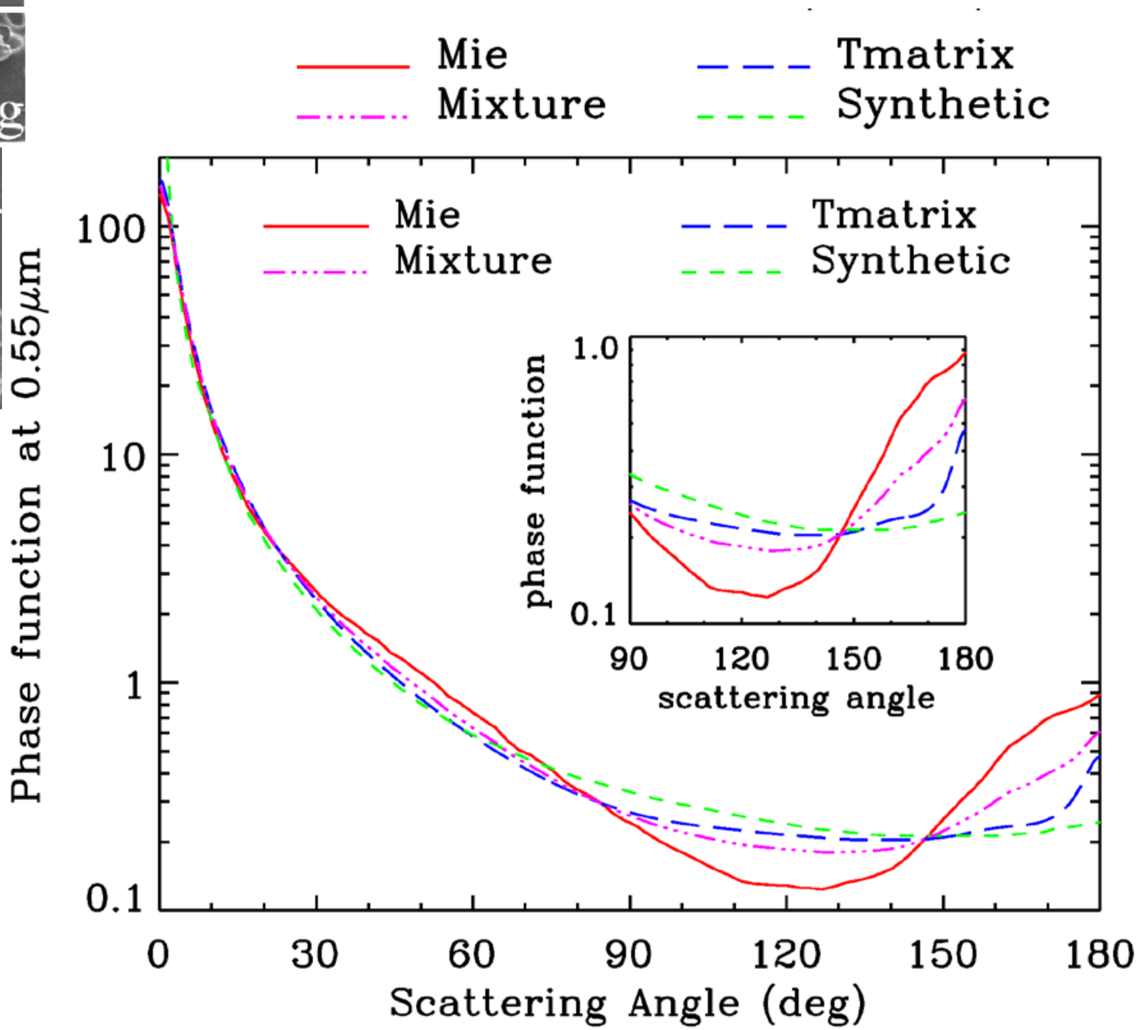

Challenges: Aerosol optical property